



LINK BUDGETING AND CHANNEL CHARACTERIZATION AT MMWAVE FREQUENCIES

Project Report

**Submitted in partial fulfilment of the requirement
for the award of the degree of**

**Bachelor of Technology
in
Electronics Engineering**

By

**Ritik Sharma
(19ELB462)**

**Anjleena Tufail
(19ELB465)**

Supervisor

Prof. Mirza Salim Beg

**DEPARTMENT OF ELECTRONICS ENGINEERING
ZAKIR HUSAIN COLLEGE OF ENGINEERING & TECHNOLOGY
ALIGARH MUSLIM UNIVERSITY ALIGARH
ALIGARH-202002 (INDIA)
May, 2023**



LINK BUDGETING AND CHANNEL CHARACTERIZATION AT MMWAVE FREQUENCIES

PROJECT REPORT

*Submitted in partial fulfilment of the
requirements for the award of the degree of*

**BACHELOR OF TECHNOLOGY
in
ELECTRONICS ENGINEERING**

by

**RITIK SHARMA
19ELB462**

**ANJLEENA TUFAIL
19ELB465**

**SUPERVISOR
PROF. MIRZA SALIM BEG**

**DEPARTMENT OF ELECTRONICS ENGINEERING
ZAKIR HUSAIN COLLEGE OF ENGINEERING & TECHNOLOGY
ALIGARH MUSLIM UNIVERSITY ALIGARH
ALIGARH-202002 (INDIA)
MAY, 2023**

STUDENTS' DECLARATION

I hereby certify that the work which is being presented in this project report entitled “**Link Budgeting and Channel Characterization at mmWave Frequencies**” in partial fulfilment of the requirements for the award of the Degree of Bachelor of Technology and submitted in the Department of Electronics Engineering of the Zakir Husain College of Engineering & Technology, Aligarh Muslim University, Aligarh is an authentic record of my own work carried out during the final year of B. Tech. under the guidance of **Prof. Mirza Salim Beg**, Department of Electronics Engineering, Aligarh Muslim University, Aligarh.

We have also checked the plagiarism of this report with the Turnitin software from Maulana Azad Library of AMU with the following details:

- Submission Date for plagiarism check: **02-May-2023**
- Submission ID for plagiarism check: **2081734275**

Note: These above details shall be available on the footer of the first page of the plagiarism report

- Similarity Index: **16%**

(**Ritik Sharma**)
Faculty Number: 19ELB462

(**Anjleena Tufail**)
Faculty Number: 19ELB465

The above statement made by students is correct to the best of my knowledge.

(**Prof. Mirza Salim Beg**)
Project Guide
Date:

ABSTRACT

This project report is an investigation into mmWave propagation characteristics, channel modeling, link budgeting and power distribution among multiple hops between Tx. and Rx. Antenna. Power measurement in Uma, Umi, Rmi scenario is also a part of this project.

The aim is to observe channel model with Power delay profiles (PDP) for both directional and omnidirectional Antenna configuration, Path loss Exponent (PLE), power spectrum, path loss plots, Outdoor to Indoor (O2I) Penetration Loss etc. at millimeters Wavelength band for both LOS and NLOS environments using a open source novel, measurement based channel simulator NYUSIM.

Obtaining this information is vital for the design and operation of future work systems for mm-wave spectrum. The project is mostly revolving around measuring the channel characterization parameters for mmWave frequencies and the path loss model in free space and other scenarios. The effect of foliage loss, the rainfall loss, building penetration loss and the effect of change in antenna polarization settings are also investigated.

Taking the advancement of Machine Learning in recent years into account, this project also studies dataset generation for a channel whose Channel Impulse Response is time varying. As measurement of transmitter power and received power using mmWaves can't be done because of unavailability of certain equipment. We have used NYUSIM for channel estimation at mmWave frequency range. Matlab script that helps in generation of this channel matrix dataset are thoroughly studied in this project. This channel matrix dataset can be further used by applying different machine learning predictive algorithms to predict future variations in the channel.

ACKNOWLEDGEMENTS

I would like to express my sincere thanks and gratitude to my supervisor **Prof. Mirza Salim Beg** for his inspiring motivation, suggestion, and guidance in the successful completion of the project on the topic “**Link Budgeting and Channel Characterization at mmWave Frequencies.**” He has always been very attentive, responsible, and supportive to me. He also helped me in doing a lot of Research and I came to know about so many new things. I am grateful to him for sparing the precious time despite all his busy schedule. He encouraged me to the highest peak and invested his time correcting my mistakes throughout my work and providing valuable suggestions. I have achieved a good amount of knowledge through this project and I humbly acknowledge a lifetime deep gratitude to him for providing me with all the facilities that I required.

(Ritik Sharma)

(Anjleena Tufail)

Date:

TABLE OF CONTENTS

	Page No
Candidate's Declaration	ii
Abstract	iii
Acknowledgements	iv
Contents	v
List of Figures	vii
List of Tables	ix
List of Symbols	x
List of Abbreviations	xi

Section No.	Title	Page No.
Chapter 1	Introduction	1
1.1	Literature Review	2
Chapter 2	Path Loss	5
Chapter 3	Effect of Rain Rate	12
Chapter 4	Foliage Loss	15
Chapter 5	Building Penetration Losses	19
Chapter 6	Impact of Antenna Polarization	23
Chapter 7	Small-Scale and Large-Scale Effects on Received Signal	26
7.1	Large- Scale Effects	26
7.2	Small- Scale Effects	27

Chapter 8	Rayleigh Distribution	30
Chapter 9	Time Delay spread	35
Chapter 10	How to generate PDP Dataset using NYUSIM?	37
10.1	Generating PDP Information using NYUSIM	37
10.2	MATLAB script for Generating PDP Dataset	38
Chapter 11	Channel Model and finding Channel Matrix	40
11.1	Channel Matrix	40
11.2	Saleh-Valenzuela Channel Model	42
11.3	MATLAB Script for finding Channel Matrix	44
Chapter 12	Verifying the Results	46
Chapter 13	Conclusion	55
	References	58

LIST OF FIGURES

Figure No.	Caption	Page No.
1.1	GUI of NYUSIM simulator	2
2.1	Free Space propagation loss	5
2.2	Free space propagation loss (log scale)	5
2.3	Path loss for Umi model	6
2.4	Small scale PDP plot for Umi model	6
2.5	Omnidirectional PDP for Umi model	6
2.6	Directional PDP for Umi model	6
2.7	Path loss for Rma model	7
2.8	Small scale PDP plot for Rma model	7
2.9	Omnidirectional PDP for Rma model	7
2.10	Directional PDP for Rma model	7
2.11	Path loss plot according to data in table 2.1	10
2.12	Received power comparison between omni-directional and directional	11
3.1	Rain attenuation	12
3.2	Atmospheric absorption	12
3.3	Power Received plot at different rain rate for directional antenna	14
4.1	NYUSIM foliage loss	16
5.1	Penetration loss	20
5.2	Frequency vs O2I loss	22
6.1	Co-Pol PDP for Directional antenna	24
6.2	X-Pol PDP for Directional antenna	24
6.3	Co-Pol PDP for Omnidirectional antenna	24

6.4	X-Pol PDP for Omnidirectional antenna	24
7.1	Small-scale and large-scale fading	28
8.1	Example of multipath propagation	30
8.2	Received signal strength in average path loss and Rayleigh fading	31
8.3	Rayleigh distributed amplitude of received signal	32
8.4	Average P_b for BPSK in Rayleigh Fading and AWGN	34
9.1	Transmission of a pulse over a multipath channel	35
9.2	Intersymbol interference (ISI)	36
11.1	Channel Matrix for M transmitting antenna and N receiving antennas	41
11.2	Multiple clusters from Multipath propagation of transmitted signal	42
12.1	Histogram for generated channel model	50
12.2	PDF for generated channel model	50
12.3	PDF for phase of the amplitude received	51
12.4	PDF for generated channel model for different T-R separation	53
12.5	Random variations in channel as shown by overlapping resultant of CIR for 2 conditions	53
13.1	BER for BPSK modulation in the generated dataset for Rayleigh Channel	57

LIST OF TABLES

Table No.	Title	Page No.
2.1	Path loss and Received power at different frequencies	9
3.1	Path loss and Received power at different frequencies while rain rate is 2.5 mm per hr	13
3.2	Path loss and Received power at different frequencies while rain rate is 7.5 mm per hr	13
3.3	Path loss and Received power at different frequencies while rain rate is 30 mm per hr	13
4.1	Path loss and Received power at different frequencies while foliage distance is 3m and attenuation is 0.4dB/m	16
4.2	Path loss and Received power at different frequencies while foliage distance is 6m and attenuation is 2dB/m	17
4.3	Path loss and Received power at different frequencies while foliage distance is 10m and attenuation is 8dB/m	17
5.1	BPL at different frequencies	21
6.1	Path loss and received power plot for directional and omni-directional antennas with co-pol and x-pol patthern	24
12.1	Channel Parameters entered in NYUSIM	47

LIST OF SYMBOLS

n	Path loss exponent
σ	Standard deviation
σ^2	Variance
d	Distance between Tx and Rx
f	Operating frequency
5G	Fifth Generation
6G	Sixth Generation
B_c	Coherence bandwidth
σ_T	RMS delay spread

LIST OF ABBREVIATIONS

mmWave	Millimeter wave
T-R	Transmitter- Receiver
LOS	Line-of-sight
NLOS	Non-Line-of-sight
SISO	Single-input single-output
MIMO	Multiple-input multiple-output
UMi	Urban microcell
UMa	Urban macro cell
RMa	Rural macro cell
PDP	Power Delay Profile
CI	Close-in
FSPL	Free space path loss
Tx	Transmitter
Rx	Receiver
GUI	Graphical user interface
RF	Radio frequency
EM	Electromagnetic
AoA	Angle of arrival
AoD	Angle of departure
PLE	Path loss exponent
AT	Atmospheric attenuation
dBm	Decibels relative to one milliwatt
PDP	Power delay profile
V-V	Vertical transmit and vertical receive
V-H	Vertical transmit and horizontal receive

BPL	Building Penetration Losses
O2I	Outdoor to indoor
Co-pol	Co-polarization
X-pol	Cross-polarization
Nt	Number of Transmitter antenna elements
Nr	Number of Receiver antenna elements
BER	Bit error rate
CIR	Channel impulse response

Chapter 1

Introduction

Today's world is seeing rapid growth in mobile services and application and it is increasing explosively. This increasing growth translates to increased requirement of data rates and traffic volume and when these demands are met than further requirement of higher bandwidth also increases. We are all aware that mmWave has the ability of offering large bandwidth and increased data speeds but there are numerous challenges, the most significant of which is that as frequency increases, signal quality suffers significantly. By studying how mmWave-length frequencies behave, we may create networks that have high density and capacity. The mmWave spectrum (30-300 GHz) is proving to be a viable candidate for new wireless applications beyond 5G. However, because of their naturally short wavelength in the range of millimeters—even small objects can easily obstruct or block them. As we already know the indoor environment contains a different number of objects on whose interaction with mmWaves can cause sufficient degradation of power which will further result in unreliable communication. The incoming signal can be blocked or can loose its strength due to various reflections, refractions, diffractions, or due to scattering from these obstacles. But the large bandwidth available at mmWavelength frequencies attracts for advantages far more than its disadvantages. In this project by doing statistical based channel modeling we want to characterize the channel parameters and further using those parameter's values determine the multi-hop link designs that will be basically required when we want to go for using higher frequencies for communication purpose using existing antenna technologies such as tight beamforming using directive antennas, mmWave backhauling, mmWave relaying etc. For measuring variations of different channel parameters with changes in T-R separations, changes in frequencies used, changes in type of foliage that was encountered, changes in rain rates, changes in NLOS and

LOS communication, changes in antenna polarization settings, changes in material while penetrating building walls, a novel mmWave channel simulator, NYUSIM, is used which has all these parameters statistically and practically measured.

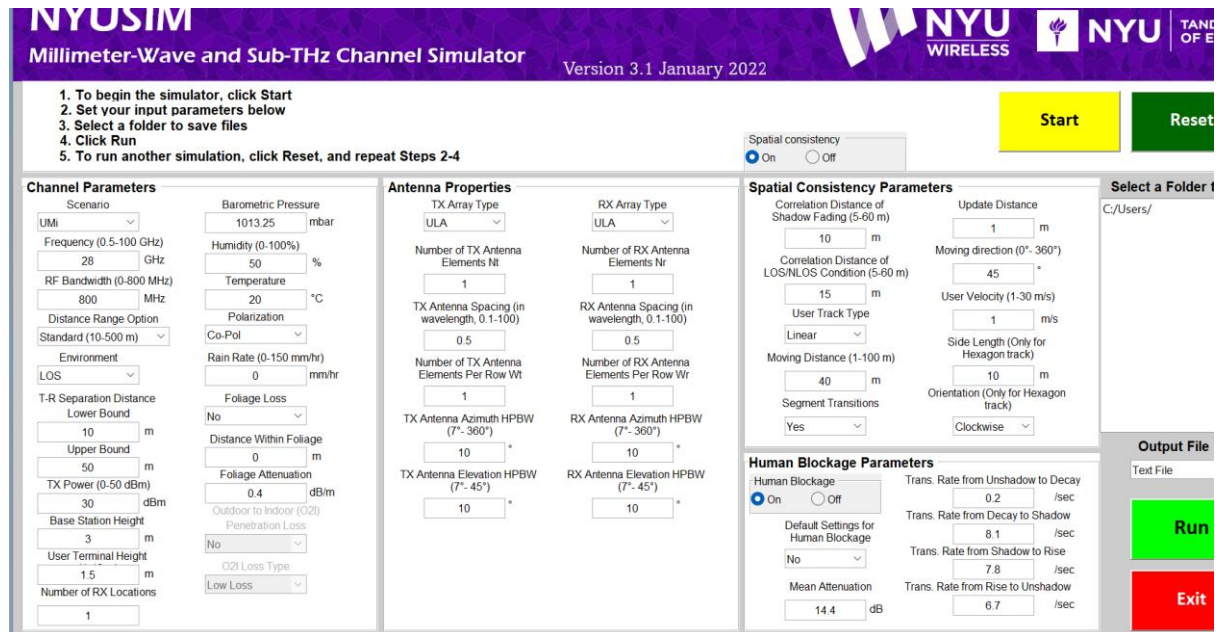


Fig 1.1 GUI of NYUSIM simulator

NYUSIM contains these measured data for propagation and reception of mmWaves using actual measured values inside the NYU campuses in Manhattan and Brooklyn [1]. The figure 1.1 is presenting the GUI of the NYUSIM simulator. It includes 49 input parameters, that are divided into 4 main categories-: Channel Parameters, Antenna Properties, Special Consistency Parameters and Human Blockage Parameters. The base file of NYUSIM is written in MATLAB and we would further extend it for generating Channel Coefficient Matrix.

1.1 Literature Review

In research paper [3], using measured data on the frequencies from 2 GHz to 73.5 GHz collected from 20 data sets with the help of different research groups, a comparison of the two large-scale propagation path loss models, in which one is the alpha-beta-gamma (ABG) model and the other one is CI (close in) path loss models in the mmWave frequency ranges, was provided. In this project, the path loss model has been studied which is implemented inside

NYUSIM and is mainly depending on Path Loss exponent and CI path loss model equation while other parameters such as Transmitter-Receiver height, foliage loss and penetration loss is not considered in the overall path loss model. The channel parameter inside the simulator are varied for a fix distance T-R separation. Data is recorded to reach to conclusions related to that parameter. As the simulator itself is novel, a lot of output that are generated required background knowledge and analysis to understand them and use them in our project's work.

In research paper [1], according to studies, the propagation of mm-waves at frequencies 28 GHz to 38 GHz for small cells will be unaffected by rain attenuation over short distances (shorter than 1 km). The result of this research has been studied in the next chapters by varying the frequencies from 25 GHz to 30 GHz at different rain rates and the comparison between them has been shown.

According to research paper [6], according to the observations taken at 28.8 GHz and 57.6 GHz vegetation loss is increased with increase in frequency and foliage depth. For the first 30 m through the foliage, the vegetation loss increases at a rate of 1.3-2.0 dB/m and nearly 0.05 dB/m after 30 m. The data relating foliage loss has been collected in next chapters using NYUSIM by varying frequencies from 0.9 GHz to 30 GHz incorporating different values of foliage attenuation and foliage distances and shows that received power reduces as more foliage (trees, plant etc) enters in the path and the power gets reduced more.

NYUSIM uses recorded data from research paper [9] to implement BPL channel model. Path loss values and Path loss exponents (PLE) for low and high BPL is recorded in next chapters. The effect of co-polarized and cross-polarized antenna are also studied and the path loss comes out to be high when cross-polarization with directional antenna is used.

Now we have realized that NYUSIM does very less calculation and throws output in terms of plots. These Plots are generated by values which were measured in real time using sophisticate equipment and by modifying NYUSIM base code, we can generate a dataset that

shows channel variations corresponding to instantaneous time. This is done by first forming a Channel Matrix for SISO systems. The same program can help us to generate Channel Matrix for MIMO (Multiple Input Multiple Output) systems. The generated Dataset can not only be used for training a communication system but also for deriving the performance of a given system using MATLAB simulations.

In research paper [13], the NYUSIM has been used to generate fading channel coefficients matrices for 6, 28 and 60 GHz channels at distances 10 m, 50 m, 100 m, and 300 m. In the further chapters a similar kind of work is being presented by generating channel coefficient matrix for SISO system at 28 GHz channel with the help of channel model- ‘Saleh Valenzuela channel model.’ A MATLAB code has been implemented to realize channel matrix. The verification of the proposed channel matrix will be done by plotting separate characteristics of the channel conditions like Histogram for generated channel model, Pdf for generated channel model and Pdf for phase of the amplitude received etc.

Chapter 2

Path Loss

Initially the work started from simulating the friis free space equation path loss on the MATLAB. free space propagation loss plots in matlab are generated to understand why the plots in the simulation were coming out to be linear. Using **fspl(distance, lambda)** function in matlab figure 2.1 is generated.

The received power, in Frii's formulas for free space propagation path loss is inversely proportional to the square of the distance between the transmitter and receiver, the path loss becomes directly proportional to square of distance. For starting the frequency used in these simulations is 900MHz.

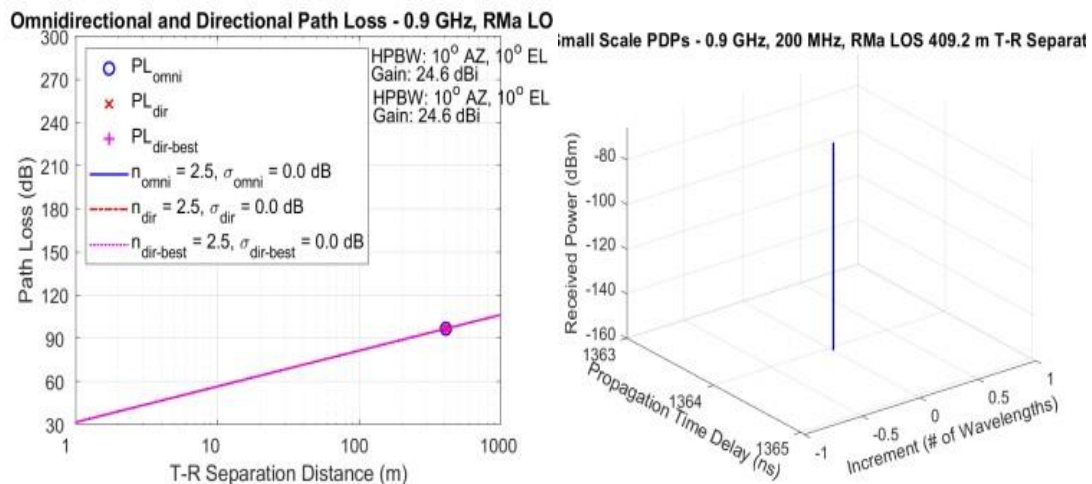


Fig.2.1 Free Space propagation path loss

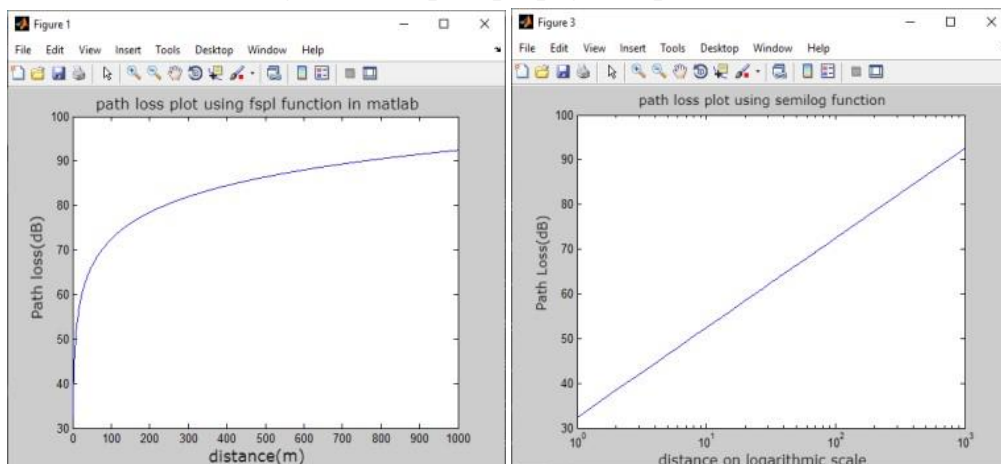


Fig. 2.2 Free space propagation path loss (log scale)

For linear characteristics the **semilog(X,Y)** function in matlab to plot semi-logarithmic curve of Path loss on dB scale against distance on logarithmic scale in figure 2.2. After that NYUSIM is used for doing the same. At first urban micro conditions were felt suitable to generate fspl plots because penetration loss, pressure, humidity, rain rate were all set to zero and LOS option was set. For starting the frequency used in these simulations is 900MHz.

Plot in figure 2.3 comes out to be same as figure 2.2 but two different lines, red and blue shows pathloss when directional antenna radiates and when omni-directional antenna radiates. The circular marks show the distance at 409.2m. It is the practical distance appeared to electromagnetic wave as propagation path between Tx and Rx.

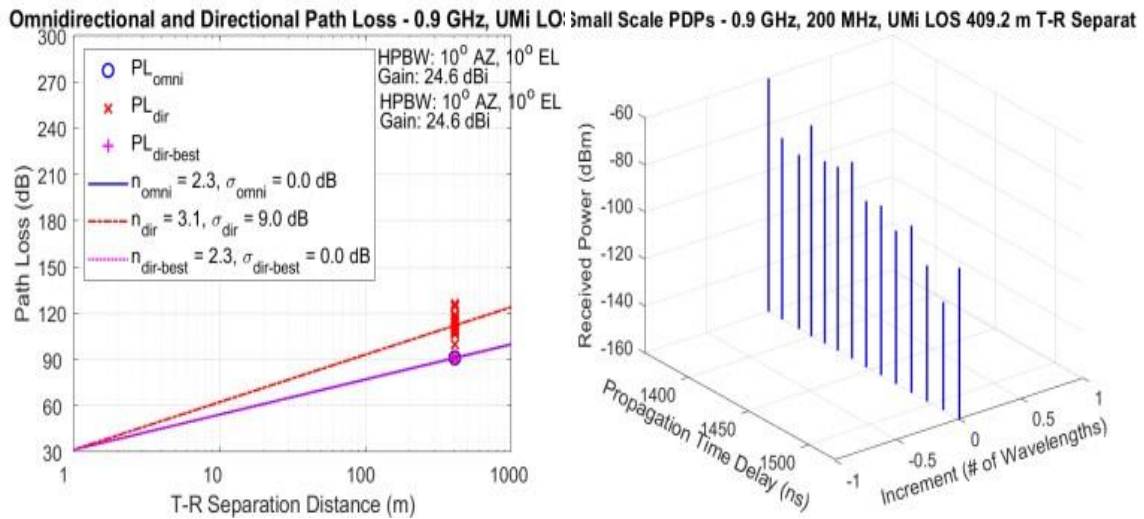


Fig. 2.3 Path loss

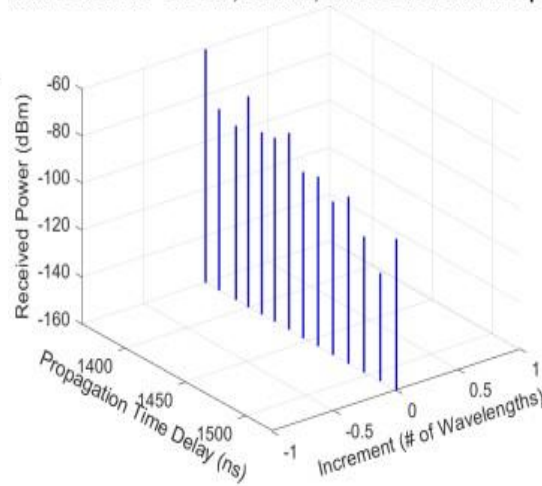


Fig. 2.4 Small scale PDP plot

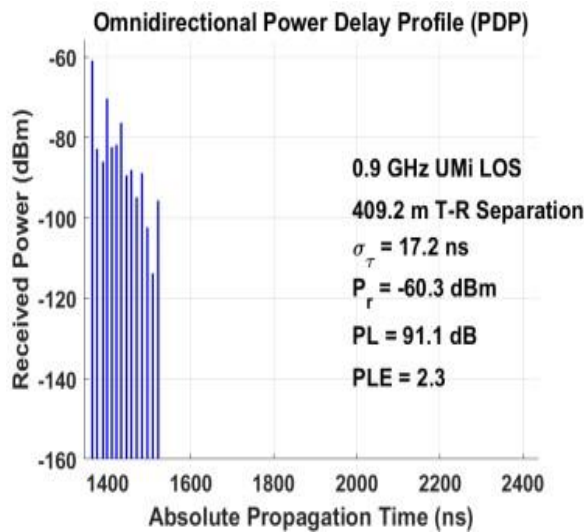


Fig. 2.5 Omnidirectional PDP

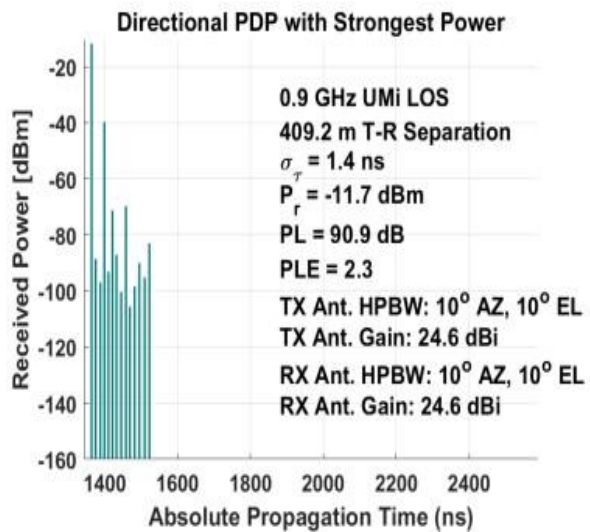


Fig. 2.6 Directional PDP

Fig. 2.4 shows the multipath components arriving at the receiver at multiple time instants and it also signifies the propagation distance between first arrived multipath component of em wave and can be given as-

$1364\text{ns} \times 3 \times 10^8 \text{ m/s} = 409.2 \text{ m}$ As we thought that it would be nice to use Umi model for fspl plot it was not a good idea because the directional antenna and omnidirectional one have different path loss plots but they both are linear as no foliage, rain , penetration loss, humidity is present.

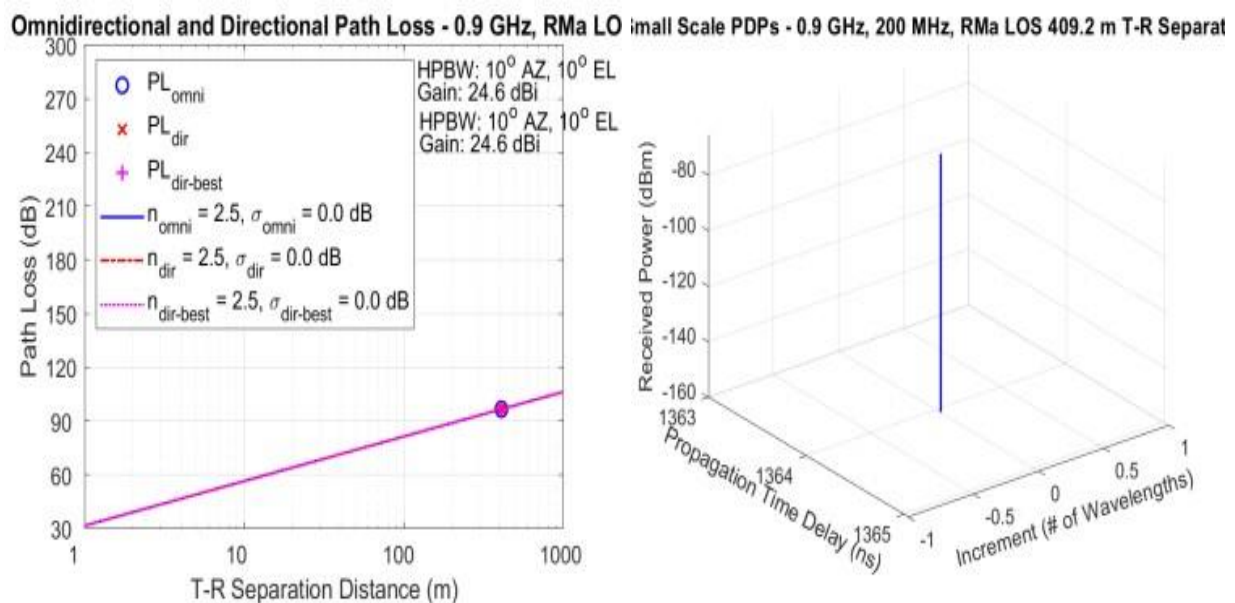


Fig.2.7 Path loss

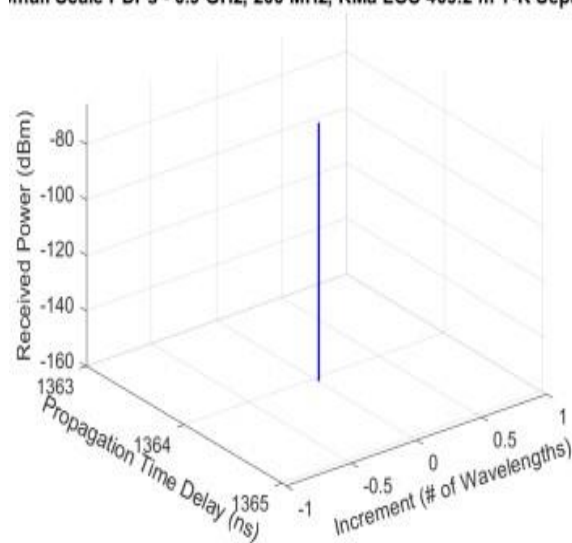


Fig.2.8 Small scale PDP

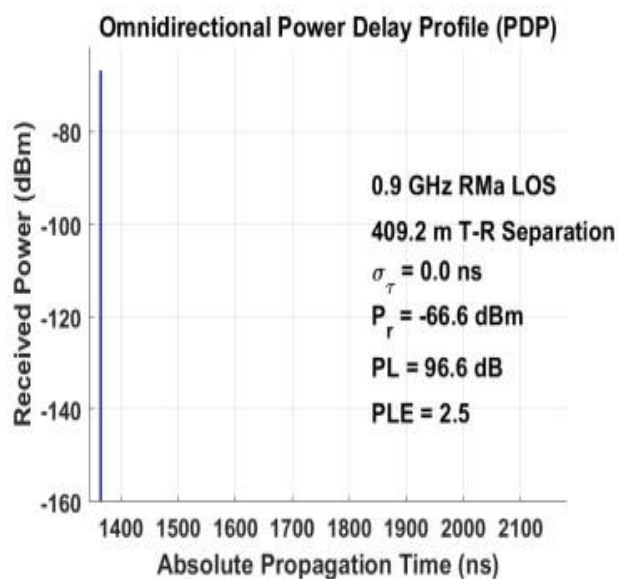


Fig. 2.9 Omnidirectional PDP

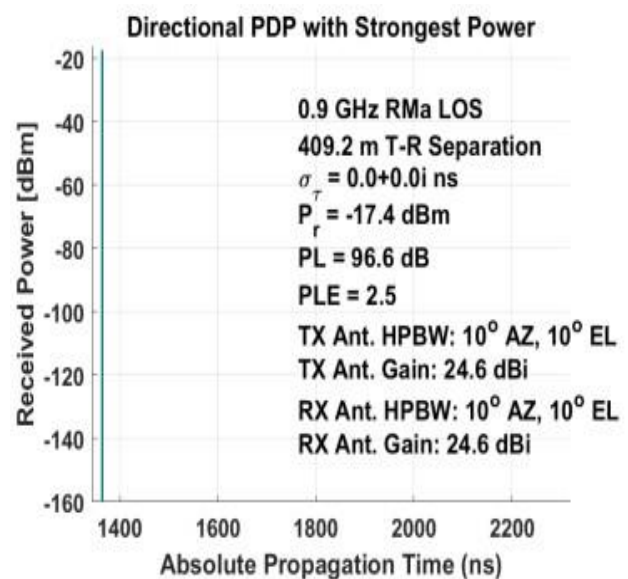


Fig. 2.10 Directional PDP

Previously Urban Micro model is used and it just means that the simulations are done and results are obtained considering urban environments. Urban environment is very complex and consists of several buildings. Through those building several reflections occurs and it leads to multiple signals delayed in time which reach at receiver. When these out of phase signals combine they lead to randomly fluctuating input signal. For making things a bit easier to understand Rma model is used where less buildings are present and signal should not have multipath components. And as expected only a single blue line is shown for the desired signal in figure 2.8. The PDP (Power Delay Profile) plots for directional and omnidirectional antennas also show a single line on the time scale showing power is received only at single instant after propagation delay.

The path loss plots in the figure 2.7 for the directional and omni-directional antennas comes out to be exact similar curves which is a straight line. That means the Rma model successfully simulated the free space path loss that occurred during propagation taking a distance of 409.2 m and losses due to pressure, foliage, humidity, rain rate and building penetration are set to zero.

In NYUSIM, the close-in free space reference distance (CI) path loss model with a 1 m anchor point and an additional attenuation term caused by various atmospheric attenuation factors is used, that is given by the equation 1[3]-

$$PL^{Cl}(f, d)[dB] = FSPL(f, 1\text{ m})[dB] + 10n \log \log_{10}\left(\frac{d}{d_0}\right) + AT[dB] + x_{\sigma}^{Cl} \quad (2.1)$$

where d_0 is the free space reference distance in metres, which is set to 1 m in the NYUSIM channel model, and f indicates the carrier frequency in GHz. The 3D T-R separation distance is denoted by d , the path loss exponent (PLE) is denoted by n .

In NYUSIM MainCode.m, users can change d_0 to any value other than 1 m, but d_0 shouldn't be greater than 5 m to ensure free space propagation within d_0 . AT is the attenuation term induced by the atmosphere, X_{σ}^{Cl} is a zero-mean Gaussian random variable with a standard

deviation _ in dB, and FSPL (f, 1 m) denotes the free space path loss in dB at a T-R separation distance of 1 m at the carrier frequency f [3]:

$$FSPL(f, 1 m)[dB] = 20 \log_{10}(\frac{4\pi f \times 10^9}{c}) = 32.4dB + 20 \log_{10}(f) \quad (2.2)$$

where c is the speed of light, and f is in GHz. The term AT can be represented by given equation [3]:

$$AT[dB] = \alpha[dB/m] \times d[m] \quad (2.3)$$

where α is the attenuation factor in dB/m for the frequency range of 1 GHz to 100 GHz, which includes the collective attenuation effects of dry air (including oxygen), water vapor, rain, and haze. d is the 3D T-R separation distance [3].

Table 2.1 Path loss and Received power at different frequencies

Frequency (GHz)	Path Loss (dB)	Power Received (directional) (dBm)	Power Received (omnidirect (dBm)
0.9	96.6	-17.4	-66.6
1	97.6	-18.3	-67.6
2	103.6	-24.4	-73.6
3	107.1	-27.9	-77.1
4	109.6	-30.4	-79.6
5	111.5	-32.3	-81.5
6	113.1	-33.9	-83.1
7	114.5	-35.3	-84.5
8	115.6	-36.4	-85.6
9	116.6	-37.4	-86.6
10	117.6	-38.3	-87.6
11	118.4	-39.2	-88.4
12	119.1	-39.9	-89.1
13	119.8	-40.6	-89.8
14	120.5	-41.3	-90.5
15	121.1	-41.9	-91.1
16	121.6	-42.4	-91.6
17	122.2	-43	-92.2
18	122.7	-43.5	-92.7
19	123.1	-43.9	-93.1
20	123.6	-44.4	-93.6
21	124	-44.8	-94
22	124.4	-45.2	-94.4
23	124.8	-45.6	-94.8
24	125.2	-46	-95.2
25	125.5	-46.3	-95.5
26	125.9	-46.7	-95.9
27	126.2	-47	-96.2
28	126.5	-47.3	-96.5
29	126.8	-47.6	-96.8
30	127.1	-47.9	-97.1

The CI model depends only on Path Loss Exponent (PLE) which is a parameter that defines the expressions, how path loss depends on the 3D separation between Tx and Rx. It is generally

denoted by n [3]. This parameter is a function of environmental conditions and the scenario in which the signal propagates. This model generally uses physical reference distances but we have assumed a standard distance in this project i.e., 1 m and ref. distance in order to compare the results for different frequencies as shown in table 2.1.(Transmitted power is 30dBm).

The initial phase of understanding the Channel Parameters box in NYUSIM GUI starts with varying the frequency from end of microwave to starting of MM wave frequency range and taking an output reading of Path loss at T-R separation of 409.2m. 30 consecutive reading are taken for monitoring path loss changes with frequency. The process was quite time consuming as we have to close the simulator GUI and then restart it, set the parameters and then making a new folder for saving simulation results.

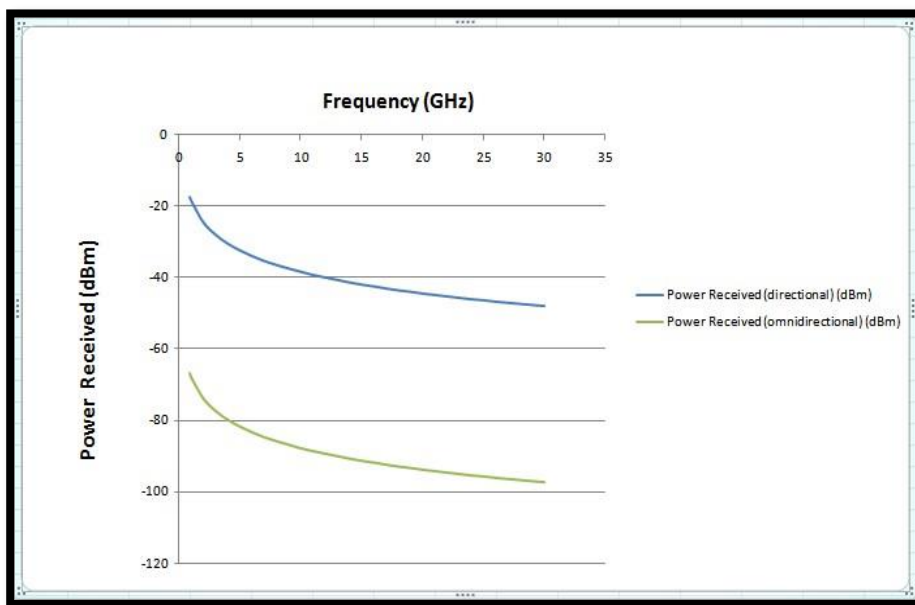


Fig.2.11 Path loss plot according to data in table 2.1

According to the fig. 2.11 which is plotted using excel according to the data in table 2.1, the path loss varies very much linearly with changes in frequency from 900 MHz to 30 GHz. In earlier project files it came out to be non-linear.

It also signifies that if further measurements were taken out then path loss came out to be an serious issue which needs to be dealt with. As we have taken a narrow transmitting beam in case of directional antenna because in Antenna Parameter GUI box Azimuth and Elevation

HPBW is set to 10° . But still the losses came out are as high as 130 dB for 30GHz EM signals.

In all the above measurements the antenna polarization is set to co-polarisation.

In the figure 2.12 attached below received power comparison between omni-directional and directional antenna is done. It can be observed that in case of directional antenna more power is received than received with the omnidirectional antenna.

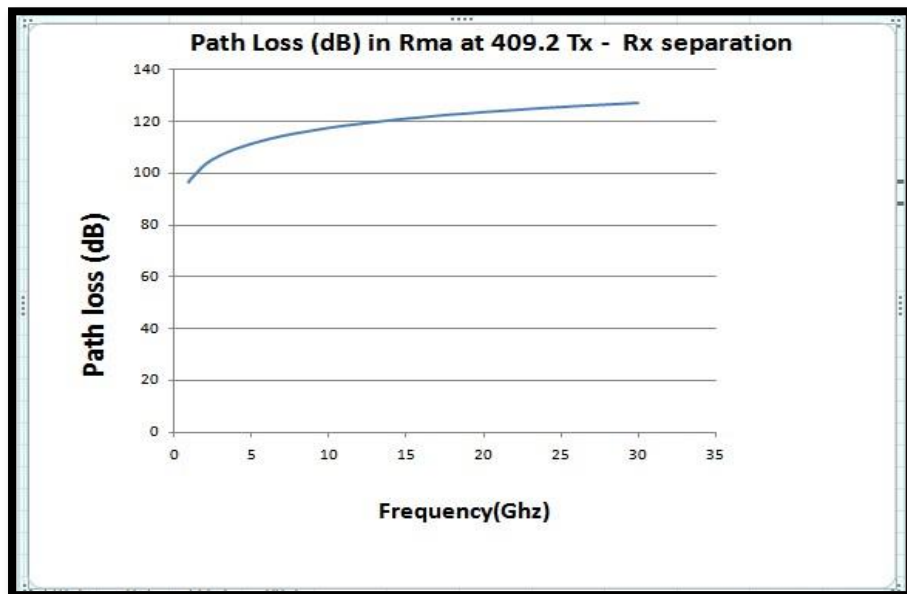


Fig. 2.12 Received power comparison between omni-directional and directional

Chapter 3

Effect of Rain Rate

In the field of wireless engineering, there is a widespread belief that the mm-wave spectrum is unusable for mobile communication due to rain and the atmosphere. However, it is evident that mm-wave cellular can get around these problems if we consider that modern urban cell sizes are on the order of 200 m[1]. Figures 3.1 and 3.2 depict the characteristics of mm's atmospheric absorption and rain attenuation of mmWave propagation [1].

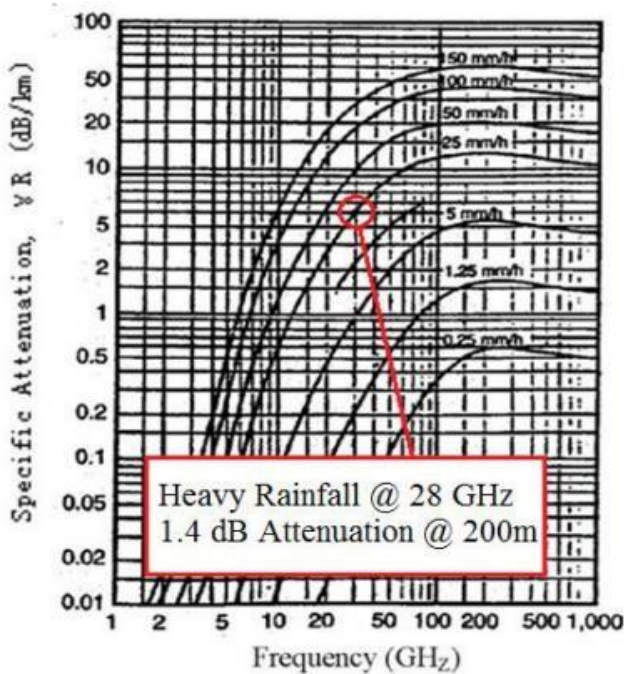


Fig. 3.1 Rain attenuation [1]

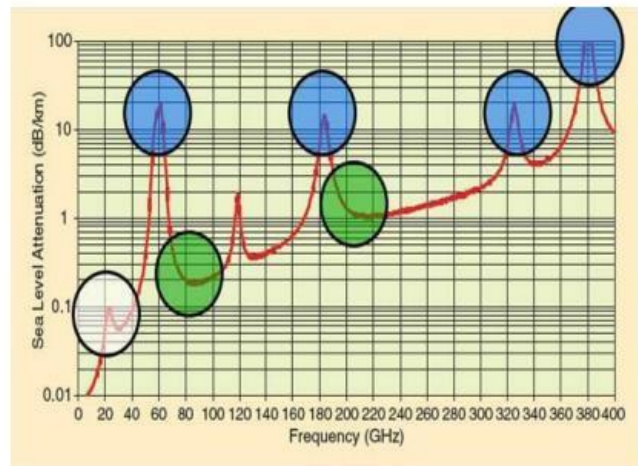


Fig. 3.2 Atmospheric absorption [1]

It is clear that atmospheric absorption, particularly at 28 GHz and 38 GHz, does not significantly increase path loss for mm-waves for cell sizes of about 200 m. Due to heavy rainfall rates of 1 inch/hr for cellular propagation at 28 GHz, only 7 dB/km of attenuation is anticipated, which equates to only 1.4 dB of attenuation over a 200 m distance. Numerous studies have shown that rain attenuation has a negligible impact on the propagation of mm-waves at 28 GHz to 38 GHz for small cells over short distances (less than 1 km) [1].

In the NYUSIM the data from the fig. 3.1 and fig. 3.2 is used and hence only the lower most window of low losses for mmWaves i.e. 25-30 GHz is used for carrying out rain-rate effect on received power simulations. The tables are attached below-

Table 3.1 Path loss and Received power at different frequencies while rain rate is 2.5 mm per hr

Rain rate 2.5			
Frequency GHz	Path Loss(dB)	Pr (Directional)	Pr (Omni-directional)
25	125.6	-46.4	-95.6
26	126	-46.8	-96
27	126.3	-47.1	-96.3
28	126.7	-47.4	-96.7
29	127	-47.8	-97
30	127.3	-48.1	-97.3

Table 3.2 Path loss and Received power at different frequencies while rain rate is 7.5 mm per hr

Rain rate 7.5			
Frequency GHz	Path Loss(dB)	Pr (Directional)	Pr(Omni-directional)
25	125.9	-46.7	-95.9
26	126.3	-47.1	-96.3
27	126.6	-47.4	-96.6
28	127	-47.8	-97
29	127.3	-48.1	-97.3
30	127.6	-48.4	-97.6

Table 3.3 Path loss and Received power at different frequencies while rain rate is 30 mm per hr

Rain rate 30			
Frequency GHz	Path Loss(dB)	Pr (Directional)	Pr(Omni-directional)
25	127.3	-48	-97.3
26	127.7	-48.5	-97.7
27	128.1	-48.9	-98.1
28	128.5	-49.3	-98.5
29	128.9	-49.7	-98.9
30	129.4	-50.1	-99.4

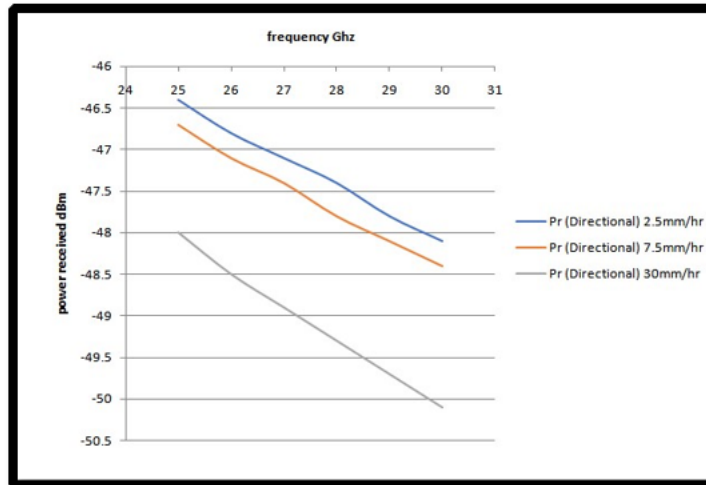


Fig. 3.3 Power Received plot at different rain rate for directional antenna

In this section LOS model in NYUSIM is selected with co-polarisation setting of antenna. All the other parameter such as Temp - 20 degree C, Pressure – 1atm and no foliage losses are set. As tight beam-forming radiation is to be considered LOS model became the absolute choice for communication at mmWave Frequencies.

Chapter 4

Foliage Loss

Outdoor urban and suburban environments frequently feature vegetation, which has an effect on the quality of a mmWave communication link due to its additional attenuation, scattering, and depolarization effects. Future mmWave radio-system design will need to take the impact of foliage on propagation into account.

Previous work has already shed light on mmWave propagation through foliage and vegetation loss, where directional antennas were used at both the base station and mobile terminals. According to [4], attenuation produced by trees at 28 GHz ranged from 16 to 18 dB in the absence of leaves to 26 to 28 dB in the presence of leaves. An attenuation factor dependent on vegetation was discovered in [5] by comparing the mean received power for line-of-sight (LOS) and non-LOS (NLOS) links, which varied from 19 dB to 26 dB at 28 GHz, depending on the different polarization schemes of the transmitted signal. Attenuation coefficients for pecan trees measured at 20 GHz ranged from 0.75 dB/m for bare trees to 2.5 dB/m for trees with foliage(leaves). The amount of vegetation loss increased with the increase in frequency and foliage depth at a rate of 1.3-2.0 dB/m for the first 30 m through the foliage and for above 30 m it is only 0.05 dB/m, according to research done at 28.8 GHz and 57.6 GHz. Attenuation experiments at 38 GHz revealed a 17 dB attenuation through an oak tree's dense canopy. The measured data showed that dry and wet leaves, respectively, could be the cause of the attenuation of 2-4 dB/m and 6-8 dB/m at 38 GHz. The above data is gathered and provided in [6]. Over the past few decades, ground reflection has also been studied at microwave bands and mmWave frequency bands.

The actual conditions in which the NYUSIM foliage loss was modeled was given in fig 4.1. Using various elevation pointing angles at both the TX and RX, complete 360° sweeps were

conducted at both the TX and RX antennas, from 10 to 40 m, for both V-V and V-H polarization configurations.[6]

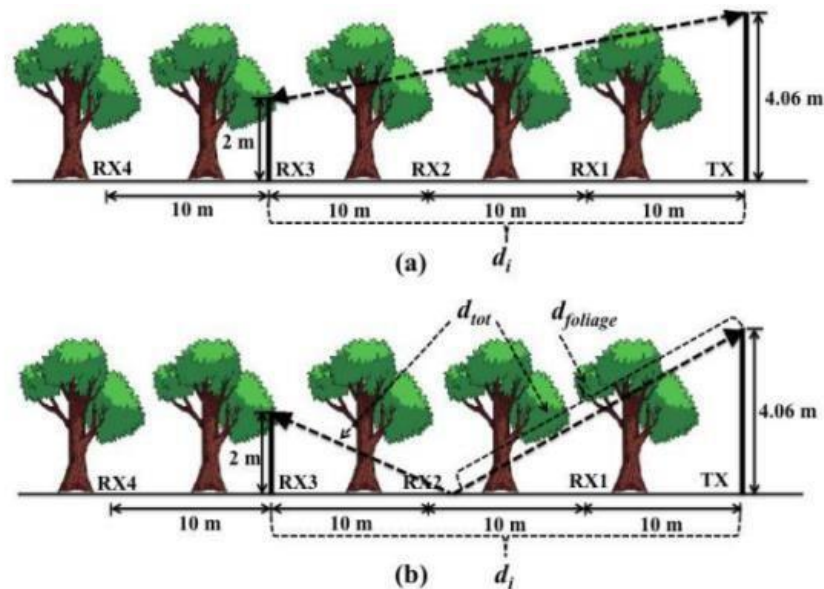


Fig.4.1 NYUSIM foliage loss [6]

Table 4.1 Path loss and Received power at different frequencies while foliage distance is 3m and attenuation is 0.4dB/m

Foliage Dist(3m), attenuation (0.4dB/m)			
Frequency GHz	Path Loss(dB)	Pr (Directional)	Pr (Omni-directional)
0.9	74.5	4.7	-44.5
1	75.4	3.8	-45.4
3	85	-5.8	-55
5	89.4	-10.2	-59.4
7	92.3	-13.1	-62.3
9	94.5	-15.3	-64.5
11	96.3	-17.1	-66.3
13	97.7	-18.5	-67.7
15	99	-19.7	-69
17	100	-20.8	-70
19	101	-21.8	-71
21	101.9	-22.7	-71.9
23	102.7	-23.5	-72.7
25	103.4	-24.2	-73.4
27	104.1	-24.9	-74.1
30	105	-25.8	-75

Table 4.2 Path loss and Received power at different frequencies while foliage distance is 6m and attenuation is 2dB/m

Foliage Dist(6m), attenuation (2dB/m)			
Frequency GHz	Path Loss(dB)	Pr (Directional)	Pr (Omni-directional)
0.9	85.3	-6.1	-55.3
1	86.2	-7	-56.2
3	95.8	-16.6	-65.8
5	100.2	-21	-70.2
7	103	-23.9	-73.1
9	105.3	-26.1	-75.3
11	107.1	-27.9	-77.1
13	108.5	-29.3	-78.5
15	109.8	-30.5	-79.8
17	110	-31.6	-80.8
19	111.8	-32.6	-81.8
21	112.7	-33.5	-82.7
23	113	-34.3	-83.5
25	114.2	-35	-84.2
27	114.9	-35.7	-84.9
30	115.8	-36.6	-85.8

Table 4.3 Path loss and Received power at different frequencies while foliage distance is 10m and attenuation is 8dB/m

Foliage Dist(10m), attenuation (8dB/m)			
Frequency GHz	Path Loss(dB)	Pr (Directional)	Pr (Omni-directional)
0.9	153.3	-74.1	-123.3
1	154.2	-75	-124.2
3	163.8	-84.6	-133.8
5	168.2	-89	-138.2
7	171.1	-91.9	-141.1
9	173.3	-94.1	-143.3
11	175.1	-95.9	-145.1
13	176.5	-97.3	-146.5
15	177.8	-98.5	-147.8
17	178.8	-99.6	-148.8
19	179.8	-100.6	-149.8
21	180.7	-101.5	-150.7
23	181.5	-102.3	-151.5
25	182.2	-103	-152.2
27	182.9	-103.7	-152.9
30	183.8	-104.6	-153.8

The data in table 4.1, 4.2 and 4.3 shows that received power reduces as more foliage (trees, plant etc) enters in the path and the power gets reduced more. In case of omnidirectional antenna, the power is reduced to as low as -160 dBm when the frequencies enters into mmWave spectrum range. But for directional antenna it is significantly low. This brings us further to a conclusion of using links which multi-hop the signals in between the T-R separation and directive beam-forming is a must in case of mmWave communication.

Chapter 5

Building Penetration Losses

A radio wave may be hampered as it moves from the sending to the receiving antenna by reflections off structures and other sizable obstructions. When numerous of these reflected portions of the wave get to the receiving antenna and obstruct the wave's reception, problems occur. In between the transmitter and receiver these reflections are within the channel and this channel is not static, it is dynamic, as there are vehicles moving, humans walking, foliage present in the direct line of sight and Man-made structures such as buildings and homes. The losses due to presence of building are known as Building Penetration Losses.

When a mobile user stands inside a building the electromagnetic power radiated by Base station antenna experiences some attenuation while penetrating the walls of the building which is known as the building penetration loss. The EM field is measured in various areas of the building where the mobile user is located and is subtracted from external EM field to determine the BPL. Building Penetration loss models are generally required nowadays because construction is going on at a large rate in a developing city or state, which are in practice, our coverage area for transmitting antennas. Different electronic and software tools are used as coverage prediction tools which must take into account the environment around the buildings which is under consideration. The following physical factors have an impact on the building penetration loss's value; their effects frequently interact with one another.

- the near environment
- the reception depth in buildings
- the incidence angle
- the reception height
- the T-R separation

- the frequency
- the nature of the materials

Another empirical statistical model is presented in [7]. Different telecom giants contributes to measuring the losses in different materials for up to 40GHz of frequencies. In [7] The building penetration loss model in accordance with [3GPP TR36.873] comprises the following parts:

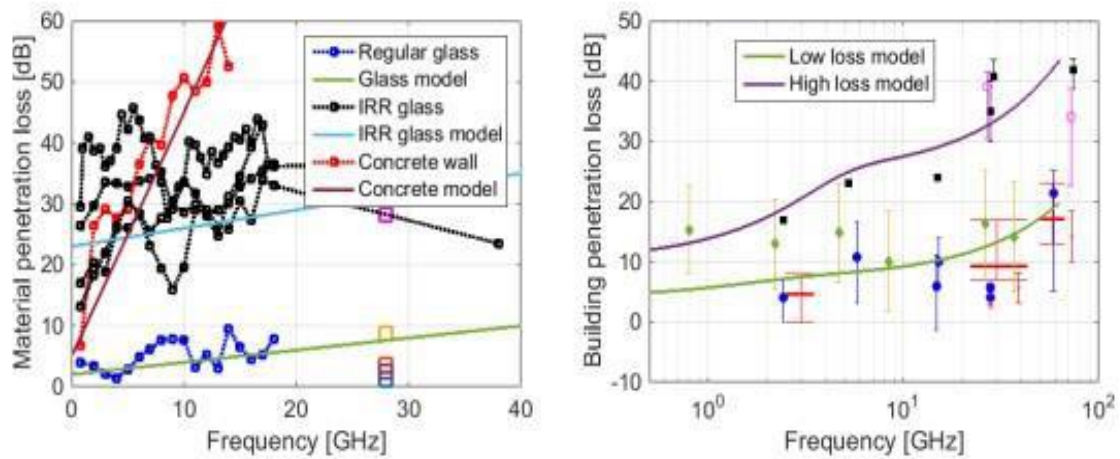
$$PL = PL_b + PL_{tw} + PL_{in} + N(0, \sigma) \quad (5.1)$$

where PL_b , the path loss given by the UMa or UMi path loss reference models

PL_{tw} , the building penetration loss through the external wall,

PL_{in} , the inside loss dependent on the depth into wall

$N(0, \sigma)$ is the standard deviation.



Comparison between the material loss model and measurements (left) and the composite penetration loss model for normal incidence and measurements (right).

Fig.5.1 Penetration loss Plots [7]

Figure 5.1(left) plots some recent measurements of penetration loss in different material. The loss patterns with frequency are, roughly speaking, linear in the first order. Measurements of the effective penetration loss for incidence angles CLOSE TO 90° are plotted in figure 5.1(right). The bars show the variance for a certain structure. The composite penetration loss figure 5.1 (right) is obtained through a statistical average of the transmission through two different materials, where the proportionate surface area of each material over the building's

façade determines the weight. A low loss (green line) and a high loss model (purple line) i.e Two variants of the model are given in [7].

$$BPL[dB] = 10\log_{10}(A + B.f^2) \quad (5.2)$$

where, f is frequency in GHz, A = 5 and B = 0.03 for low loss buildings, and A = 10 and B = 5 for high loss buildings [7].

Table 5.1 BPL at different frequencies

Frequency (GHz)	Outdoor to indoor low loss					Outdoor to indoor high loss				
	Pr (omni- direc.) (dBm)	Pr (direc.) (dBm)	O2I (Low)	PL (dB)	PLE	Pr (omni- direc.) (dBm)	Pr (direc.) (dBm)	O2I (High)	PL (dB)	PLE
1	-53.2	-4.0	-3.8	83.2	2.6	-49.4	-0.2	-1.8	79.4	2.4
3	-58.9	-9.7	-1.8	88.9	2.4	-64.5	-15.3	3.9	94.6	2.7
5	-63.7	-14.5	-1.4	93.7	2.5	-72.9	-23.7	7.8	102.9	2.9
7	-67.1	-17.9	-0.9	97.1	2.5	-78.6	-29.4	10.5	108.6	3.1
9	-69.9	-20.7	-0.3	99.9	2.5	-82.9	-33.7	12.6	112.9	3.2
11	-72.3	-23.1	0.3	102.3	2.6	-86.3	-37.1	14.3	116.3	3.3
13	-74.4	-25.2	1.0	104.4	2.6	-89.2	-40.0	15.8	119.2	3.4
15	-76.3	-27.1	1.7	106.3	2.6	-91.7	-42.5	17.0	121.7	3.4
17	-78.1	-28.9	2.3	108.1	2.7	-93.8	-44.6	18.1	123.9	3.5
19	-79.7	-30.5	3.0	109.7	2.7	-95.8	-46.6	19.0	125.8	3.5
21	-81.2	-32.0	3.6	111.2	2.7	-97.5	-48.3	19.9	127.5	3.6
23	-82.6	-33.4	4.2	112.6	2.8	-99.1	-49.9	20.7	129.1	3.6
25	-83.8	-34.6	4.7	113.8	2.8	-100.5	-51.3	21.4	130.5	3.7
28	-85.6	-36.4	5.5	115.6	2.8	-102.5	-53.3	22.4	132.5	3.7
30	-86.7	-37.5	6.0	116.7	2.8	-103.7	-54.5	23.0	133.7	3.7

Table 5.1 gives the data of simulations ran on NYUSIM for BPL calculations. NYUSIM uses recorded data in [9] to implement BPL channel model in the software. Path loss and Path loss exponent for low and high BPL is given in Table 5.1. As the frequency is increased the O2I(Outdoor to Indoor) losses are also increased and the path loss exponent is also increased as it takes into account the foliage and building in the surrounding.

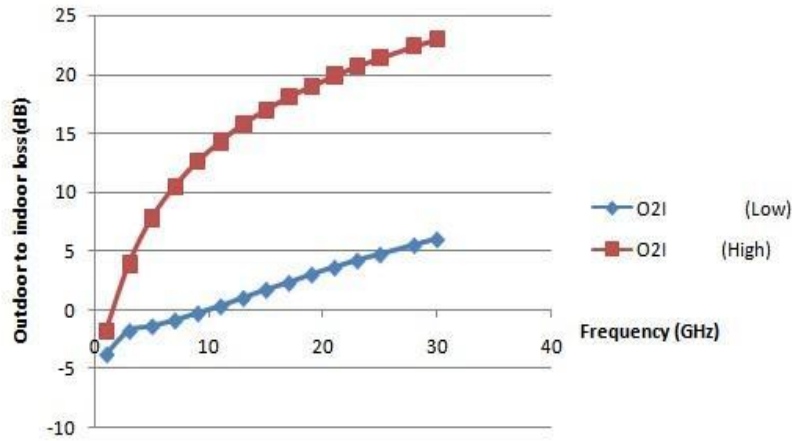


Fig. 5.2 Frequency vs O2I loss

Fig 5.2 shows the relation Frequency vs O2I. All these observations are taken for Rural macro model, T-R separation of 83.3 metres, transmission power 30dBm, LOS condition and for cross polarization. For observing more data when LOS condition is changed to NLOS condition there is no change in O2I loss. Similarly for changing the co-polarized antenna system to cross-polarized system no change in O2I loss is observed. Similarly for Umi, Uma, Rma and Inh the values of the O2I losses are same. As the model for BPL implemented in NYUSIM is based on [7] so the other variables like angle of refraction, cross-polarized or co-polarized system and no. of buildings can't be changed for observing variations in O2I losses.

As there are number of parameters which affect the Building Penetration Losses but NYUSIM only accounts for the material in broadly two figures which are high and low penetration losses. The variations according to T-R height, Angle of penetration, penetration depth and particularly different materials like concrete, sand, bricks etc aren't specifically addressed in NYUSIM.

Chapter 6

Impact of Antenna Polarization

The millimeter wave is claimed to be a key invention to address the rapidly increasing wireless demand for mobile traffic with its enormous bandwidth [10]. But the line-of-sight (LOS) and associated weather conditions, in which the path loss takes various atmospheric weather conditions into account, have a bad impact on the system performance even though the mmWave frequencies fulfill the need for more bandwidth [11]. The polarizations of electromagnetic fields produced by antennas would also have an impact on the mmWaves channel characteristics and the system performance. The dipole of an antenna is what determines its polarization. The electromagnetic field and the radio waves that the antenna transmits through space are both impacted by this orientation, or polarization. The positioning of various transmitting and receiving objects in system networks results in narrow beam radiation patterns like Co-pol and X-pol. When the two dipoles of an antenna are pointed in the same direction, this is known as copolarization. Therefore, cross-polarization occurs when the dipoles of an antenna take the form of a plus (+) or an x. In other words, they are 90 degrees apart from one another. Signal decorrelation, which is made possible by a 90-degree orientation, helps to reduce interference for signals that are received. One of the biggest benefits of cross-polarized antennas is signal decorrelation. We have used three different mmWave frequency bands; 0.9GHz, 15GHz and 30GHz in order to observe the impact of Co-pol and X-pol in NYUSIM channel modeling. First we used Rma scenario as it is easily understandable than Umi scenario which is having multiple buildings, trees and multiple obstacles and then by taking Uma scenario also the impact of co-pol and x-pol has been observed. Its impact on path loss, received power, and path loss exponent (PLE) to understand the polarization model of the mmWave, then Umi scenario is used for observation.

Table 6.1 Path loss and received power plot for directional and omni-directional antennas with co-pol and x-pol pattrhern

Co-pol,				
Frequency GHz	Path Loss(dB)	Pr (Directional)	Pr (Omni-directional)	
0.9	73.3	5.9	-43.3	
15	97.8	-18.5	-67.8	
30	103.8	-24.6	-73.8	
x-pol,				
Frequency GHz	Path Loss(directional)	Pr (Directional)	Path Loss(Omni-directional)	Pr (Omni-directional)
0.9	84.9	-5.7	73.3	-54.9
15	110.8	-31.5	97.8	-80.8
30	118.3	-39.1	103.8	-88.3

The table 6.1 is listing the path loss and received power in case of directional and omni-directional antennas with two different radiation patterns, co-pol and x-pol. From the table we can observe that path losses for co-pol directional and omni-directional antennas are the same but in case of x-pol radiation pattern path loss is different for directional and omni-directional antennas.

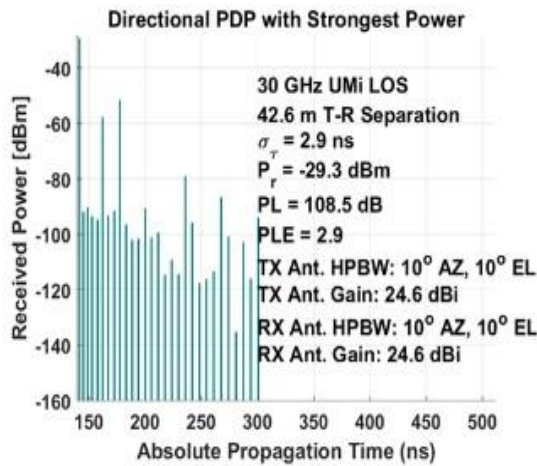


Fig. 6.1 Co-Pol PDP

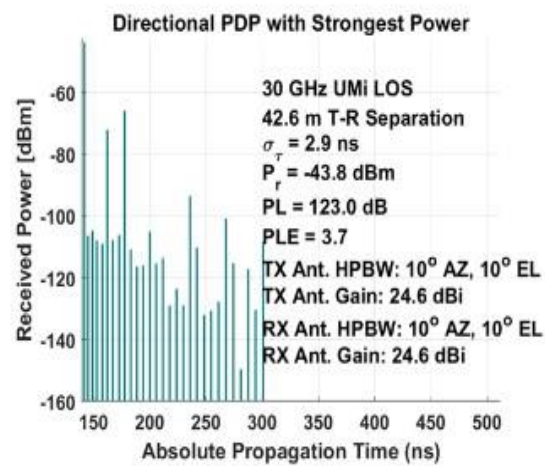


Fig. 6.2 X-Pol PDP

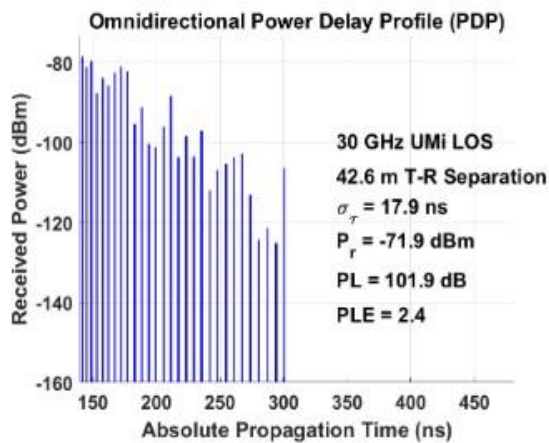


Fig. 6.3 Co-Pol PDP

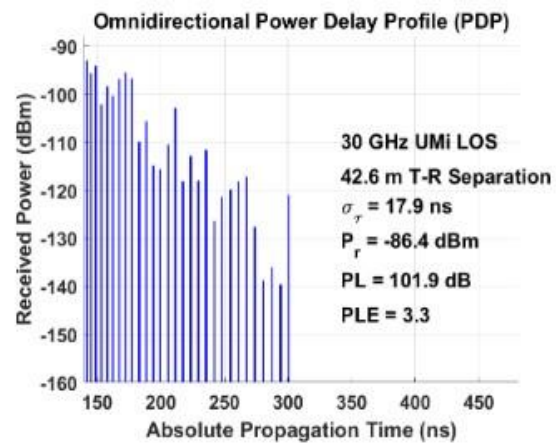


Fig. 6.4 X-Pol PDP

Both Figures 6.1 and 6.2 illustrate the effect of the change of polarization from co-pol to x-pol in terms of path loss and power received at 30GHz frequency band for directional antennas and we can observe by comparing both the graphs that the path loss gets increased and received power decreased by changing polarization from co-pol to x-pol because path loss depends on path loss exponent (PLE), can be seen in close-in free space reference distance (CI) path loss model and it is increased from 2.9 to 3.7 when polarization is changed from co-pol to x-pol and we know that PLE mainly depends on environment, propagation channel, the distance between transmitter and the receiver, the height of antenna and location of antennas. But in the case of omni- directional antennas as shown in Fig. 6.3 and 6.4 the path loss values are observed to be the same and received power is decreased as PLE is increased from 2.4 to 3.3. Friis equation can be modified to accommodate different environments, on the reason that the received power decreases as the n th power of distance as we can see from the given received power equation; where the parameter n is the *path-loss exponent (PLE)* that holds constant values depending on the environment and the antenna parameters that is being used. So that is why the received power is decreased when an increase in PLE [12].

$$P_r(d) = P_t \frac{G_t G_r \lambda^2}{(4\pi)^2 d^n L} \quad (6.1)$$

where, P_r is the power at the receiving antenna, P_t is the output power of the transmitting antenna, G_r is the gain of the receiving antenna, G_t is the gain of the transmitting antenna, d is the distance between the antennas, L is the system or hardware loss factor.

Chapter 7

Small-Scale and Large-Scale Effects on Received Signal

When the wireless signal travelling inside a wireless channel, it travels through different scenarios and encounters various obstacles such as buildings, trees, vehicles, walking crowd or other signals which results in the signal to diffract, reflect, or scatter. These causes distortion in the signal and the strength. It leads to fluctuations in the amplitude, phase, or arrival time of the signal at the receiver. The quality of the received signal power attenuates due to multipath propagation, changes in the propagation environment, atmospheric conditions, and the movement of different entities in the transmission path. This phenomenon is called Fading that impacts the performance of the received signal in telecommunication particularly those that operate in high frequency bands. It is divided into 2 types for better understanding in eliminating the negative impact of fading:-

7.1 Large-Scale Fading

Large-scale fading occurs in the wireless communication system when the received signal power is attenuated or reduced gradually due to obstacles present between the transmitter and receiver. It is encountered when the signal is propagated over a large distance typically on the order of meters or kilometres that is much larger than the wavelength of the signal. Large scale fading affects the entire signal whereas small signal affects only certain bits or symbols. It is a slow-varying phenomenon that changes throughout time scales of seconds to minutes. The most popular model for large-scale fading, the Friis free space path loss equation, determines the Path loss that calculates the received power depending on the transmitted power, the separation between the transmitter and receiver, and the gain of the transmitted and received

antennas. Path loss is basically the attenuation of the signal power as the signal travels from a transmitter to a receiver.

Path loss can be minimised by increase in transmission power, or by employing directional antennas or high-gain antennas to increase the received power or by decreasing the distance between transmitter and receiver.

7.2 Small-Scale Fading

Small-scale fading affects wireless transmission frequently. When a signal is delivered from a transmitter to a receiver, it might take several different paths because of atmospheric conditions and environmental factors like reflection, diffraction, and scattering. It is caused by Multipath components of the received signal and these multipath components results in distortion to the signal with different amplitude and phases. Small-scale fading occurs over short distances, such as a few centimetres to a few meters and on a time scale of microseconds to milliseconds. Rayleigh fading is a type of small-scale fading in which the signal received at the receiver is from different multiple paths with random amplitude and phases when there is no line of sight. The distribution of the signal power follows a Rayleigh distribution.

So, it is a rapid fluctuation of received signal strength when receiver moves over short distance of the order of the wavelength of the signal.

The fig. 7.1 has been generated by modifying the Base code of NYUSIM simulator in MATLAB. The red line shows the mean path loss curve representing large scale effect. The blue is representing the small scale effect showing the rapid fluctuations in the received power of the signal over short distances.

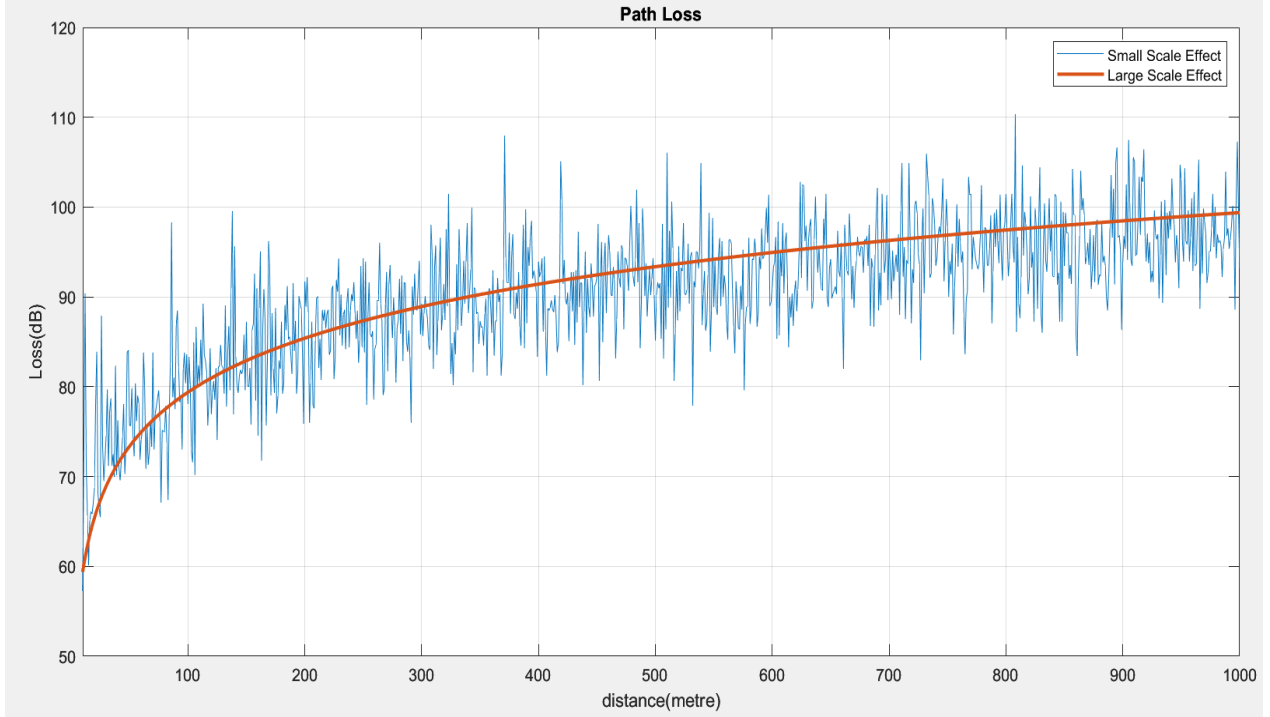


Fig. 7.1 Small-scale and large-scale fading effect

The MATLAB script to generate the small-scale and large-scale effects has been attached below. To plot the effect of small-scale and large-scale fading, first we loaded the mat file ‘dirpdpfading.mat’ in which the received power values corresponding to distances from 10m to 1000m are stored. After that each simulation run number for each distance i.e., 10-1000m has been loaded. Then received power has been calculated by converting all the values to watt from dB and multiplying it with phase of the signal that comes out to be in a complex matrix. By finding resultant received power from complex form, the path loss has been calculated and plotted with respect to distance.

Path loss for 28GHz using MATLAB's fspl function has been calculated and scaled down to show the relation between two plots. After scaling down, the path loss calculated using fspl function is plotted over the path loss plot obtained from NYUSIM data as shown in fig. 7.1.

```

small_scale_effects.m  normalised_histogram.m  getChannelMatrixCopolSinglepoint.m  no_of_si
1  clc
2  clear all; close all;
3  % initialising filename variable for loading the received power
4  % values corresponding to distances from 10m to 1000m
5  filename='dirpdpfading.mat';
6  foldername='D:\NYUSIM_V31_WIN_package\NYUSIM Base Code';
7  % loading the filename variable data
8  myfile=fullfile(foldername,filename);
9  load(myfile);
10 % loading each simulation run number for each distance, 10-1000m
11 SimNum = unique(dirpdp_contentfading(:,2));
12 % initialising matrix variable
13 A={};
14 Hf_pvs = cell(1,length(SimNum));
15 % calculating received power from PDP data
16 for id = 1:length(SimNum)
17     clear Idx; Idx = find(dirpdp_contentfading(:,2)==SimNum(id));
18     Hf_temp = sum(sqrt(10.^(dirpdp_contentfading(Idx,4)./10)) ...
19         .*exp(1i.*dirpdp_contentfading(Idx,5)));
20     % appending to A matrix
21     A = [A; Hf_temp];
22     Hf_pvs{1,id} = Hf_temp;
23 end
24 % converting cell type to matrix
25 Amp=cell2mat(Hf_pvs);
26 % measuring size of matrix
27 [r,c]=size(Amp);
28 for i=1:c
29     A=[real(Amp(1,i)),imag(Amp(1,i))];
30     % calculating resultant received power
31     resultant(i)=sqrt(A(1,1)^2 + A(1,2)^2);
32 end
33 % x axis values for Path Loss plot
34 xtemp=[10:1000];
35 % plotting path loss values for the data from NYUSIM
36 figure(1);
37 % converting dBm to Watts
38 pt=sqrt(10^(40/10));
39 % calculating path loss
40 PL=pt./resultant;
41 % plotting path loss vs distance
42 plot(xtemp,10*log10(PL));
43 xlim([10 1000]);
44 hold on
45 % initialise frequency and speed values for calculating wavelength
46 c=3e8;
47 f=28e9;
48 lambda=c/f;
49 i=1;
50 % calculating path loss for 28GHz using MATLAB's fspl function
51 for r=10:1000
52     pl_array(i)=fspl(r,lambda);
53     i=i+1;
54 end
55 % scaling down the losses to show relation between two plots
56 for i=1:991
57     pl_array(i)=pl_array(i)-22;
58 end
59 % plotting the path loss calculated using fspl function over
60 % the path loss plot obtained from NYUSIM data
61 figure(1);
62 plot(xtemp,pl_array,'Linewidth',2)
63 grid on
64 legend('Small Scale Effect','Large Scale Effect');
65 xlabel('distance(metre)');
66 ylabel('Loss(dB)');
67 title('Path Loss');

```

Script 7.1 MATLAB script to generate small- scale and large scale- effect

Chapter 8

Rayleigh Distribution

When a signal is transmitted through a transmitting antenna at a certain frequency, the signal sent by transmitting antenna travels inside wireless channel. In practical cases the wireless channel is time variant and different entities moves inside the channel, its properties may vary with time. It may include running vehicles, walking crowd and breeze shaken trees etc. These variations give rise to different multipath propagation of the transmitted signal at different time instants and lead to distortion in received signal and results in Rayleigh fading. Eventually degradation in the performance of a communication system.

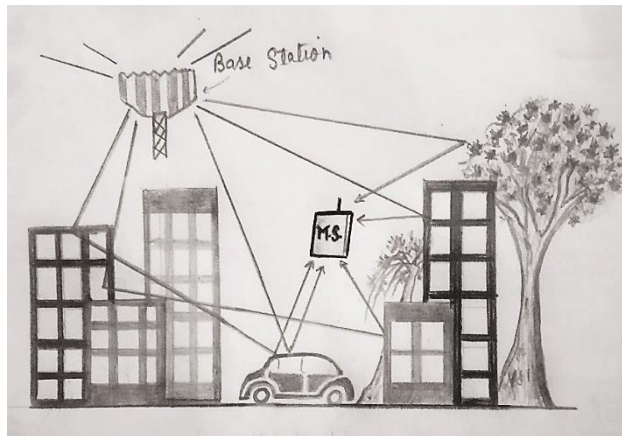


Fig. 8.1 Example of multipath propagation

Due to Multipath propagation, multiple components of transmitted signal are received and the path of the scattered signal change which introduces variations in amplitude and phase randomly of the constituent signals. When these multipath waves move back and forth due to the buildings, trees and houses as shown in Fig. 8.1, they make standing-wave pairs in space [18]. The pairs of standing waves are added together and form an irregular wave-fading structure. When a mobile unit is stationary, its receiver only receives a signal strength at that location, resulting in a constant signal strength. The fading structure of the wave in space is

received when the mobile unit is not stationary but moving. As the vehicle moves, recorded fading becomes faster.

Rayleigh fading is a type of small-scale fading that occurs in wireless communication systems when there is no line-of-sight path between the transmitter and receiver. When there is not a clear line of sight between the transmitter and receiver and there are lots of buildings and other objects in the way, then the signal is weakened, reflected, refracted, and diffracted. The numerous particles in the atmosphere also leads to Rayleigh fading. As Rayleigh fading is a small-scale effect; it is overlayed on the environment's bulk properties, such as on path loss and shadowing, as the fig. 8.2 shows. The distribution of signal strength in Rayleigh fading follows a Rayleigh distribution, which is a statistical model that describes the probability distribution of the amplitude of a signal that has undergone random attenuation. The Rayleigh distribution is characterized by a probability density function that is proportional to the square of the amplitude. Received signal amplitude (envelope) will change as random variable i.e., its pdf has Rayleigh distribution. Phase of the received signal will change randomly but with uniform distribution between 0 to 2π .

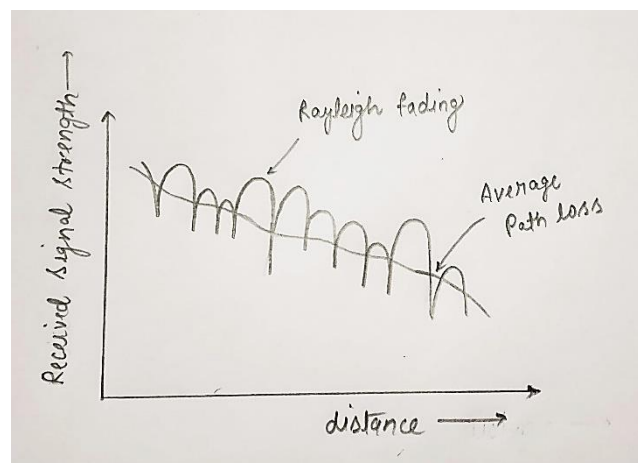


Fig. 8.2 Received signal strength in average path loss and Rayleigh fading [18]

The resultant received signal at the antenna is given by the resultant complex phasor which can be written as-

$$r.e^{j\theta} = x+j.y \quad (8.1)$$

If it is assumed that individual values of θ are independent and uniformly distributed then it can be shown using Central limit theorem that x and y are gaussian random variable with zero mean. Then the received signal may be interpreted as the sum of two amplitude modulated carrier signals in phase quadrature with randomly varying envelope. Because of this, it can be concluded that the envelope of the resultant received carrier has an amplitude with a Rayleigh probability distribution and given by the equation -:

$$\frac{x}{\sigma^2} e^{-\frac{x^2}{2\sigma^2}} \quad (8.2)$$

Where σ^2 is the variance of each of the Gaussian variables x and y .

The peak value of the Rayleigh probability density function is $\frac{1}{\sigma\sqrt{e}}$ and it occurs at $x=\sigma$, hence σ is the most probable value i.e., mode. Thus the resultant carrier envelope (x) has only positive values.

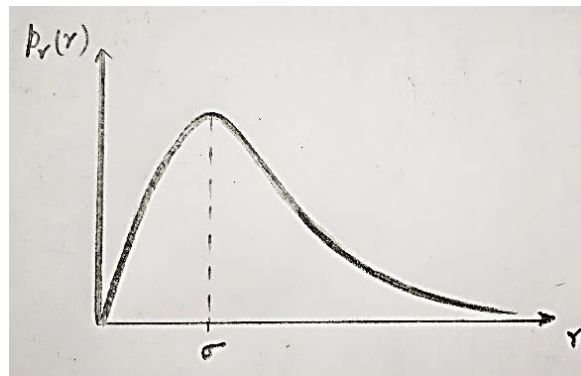


Fig. 8.3 Rayleigh distributed amplitude of received signal

The mean or the expected value of the Rayleigh envelope is $E(x) = \sigma\sqrt{\frac{\pi}{2}}$.

The mean square value of Rayleigh envelope is $E(x^2) = 2 \sigma^2$.

The median value of Rayleigh envelope is 1.177σ .

In a fading environment, the strength of the received signal at the receiver is not constant, but varies randomly. The randomness of the received signal strength is represented by the random variable γ_s (bit energy), which has a probability distribution $P_{\gamma_s}(\gamma)$. The signal power $P_s(\gamma_s)$ is also random, because it depends on the value of γ_s , which is itself random. So, the probability of bit error P_b is also random and depends on both the value of γ_s and the modulation scheme used. In AWGN (Additive white Gaussian noise), the probability of symbol error depends on the received signal-to-noise ratio (SNR), which is proportional to γ_s . The performance of a modulation scheme in AWGN can be predicted using the SNR, which is a deterministic parameter. However, in a fading environment, the performance of a modulation scheme depends on the rate of change of the fading. If the fading changes rapidly, then the bit error probability may be higher than if the fading changes slowly. Therefore, the performance metric for a random γ_s depends on the rate of change of the fading.

Comparing the bit error probability of different modulation schemes in AWGN and fading environments can help in selecting the most appropriate modulation scheme for a given wireless communication system. In AWGN channels, the bit error probability for binary phase shift keying (PSK), frequency shift keying (FSK), and differential PSK (DPSK) decreases exponentially with increasing bit energy γ_b . This is because in an AWGN channel, the received signal is only affected by additive white Gaussian noise, which is a random process that adds noise to the received signal. Therefore, increasing the bit energy γ_b means that the signal-to-noise ratio (SNR) increases, which leads to a decrease in the bit error probability. However, in fading channels, the bit error probability for all modulation types, including nonbinary modulation, decreases linearly with increasing bit energy γ_b . This is because in a fading channel, the received signal is affected not only by noise, but also by the random variations in the channel caused by fading. Therefore, increasing the bit energy γ_b may not lead to a

proportional increase in the SNR, since the effects of fading may still cause errors in the received signal. As a result, to maintain a given bit error probability P_b , the power required in fading channels is much higher than required in AWGN channels [20]. This study has been verified in chapter 13.

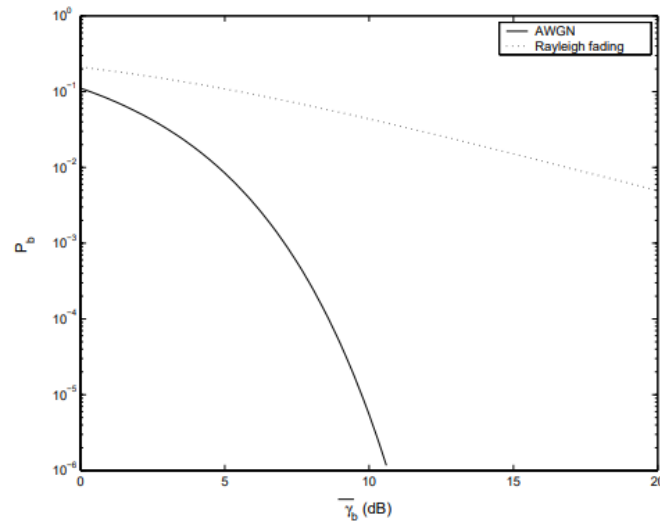


Fig. 8.4 Average P_b for BPSK in Rayleigh Fading and AWGN channel [20]

Chapter 9

Time Delay spread

In telecommunications, due to multipath phenomenon, the signal arriving at a receiver will be from different paths. As each path of the signal propagation has a different path length, the time of arrival for each path is different. The transmission of one narrow pulse results in reception of train of pulses at different moments. Delay spread can be defined as the difference between the time of arrival of the earliest component of multipath (usually the line-of-sight component) and the time of arrival of the last multipath component. The measure of the channel's average delay spread in seconds is known as RMS Delay Spread, (root-mean-square) value of the delay of multipath reflections, weighted proportional to the power in the reflected multipath components. Time domain parameter is rms delay spread σ_T and the frequency domain parameter is coherence bandwidth B_c .

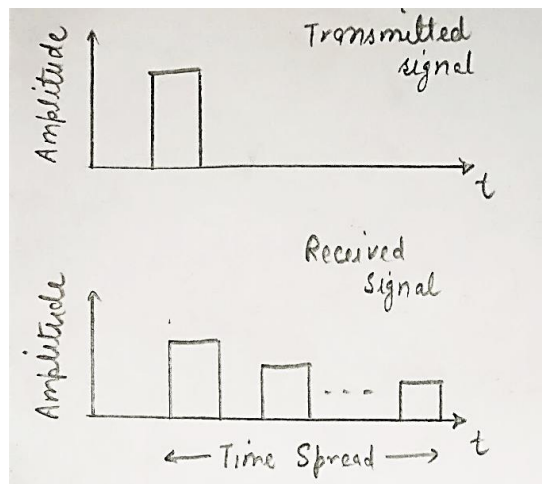


Fig. 9.1 Transmission of a pulse over a multipath channel

Multipath time delay spread is a major limiting factor in operation of a high bit rate systems. If the time delay spread is less than the time duration of transmitted pulse ($T_m \ll T$), then the multipath components that are received, roughly overlapping each other. Resulting constructive and destructive interference causes narrowband fading of the pulse, but there is little time spreading of the pulse and therefore little interference with a subsequent transmitted

pulse. But when the time delay spread becomes large ($T_m \gg T$), these multipath components interfere with the next subsequently transmitted pulses (shown with the dashed lines in the fig. 9.2) and leads to lot of Intersymbol interference (ISI) and causes wideband fading. Thereby a degradation in the system performance.

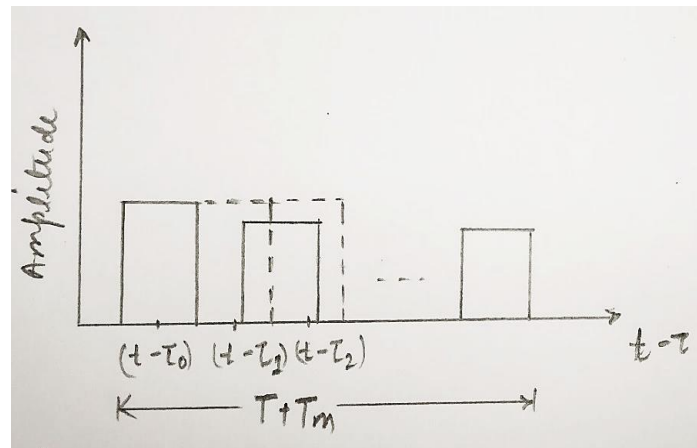


Fig. 9.2 Intersymbol interference (ISI)

Higher the time delay spread in the channel, the more sophisticated receiver signal processing would be required. Value of time delay spread depends upon the environment where it is being measured. For an indoor wireless system (where transmitter and receiver are both located inside a house), the average value of time delay spread will be lower, due to smaller distances of propagation. For an outdoor wireless system, such as in cellular mobile radio systems, the average value of time delay spread will be higher, due to larger distances of propagation [18].

When time delay spread is very small -:

- Very small amount of ISI is present
- signal bandwidth \ll channel coherence bandwidth
- Flat fading

When time delay spread is very high -:

- Very large amount of ISI
- Signal bandwidth \gg channel coherence bandwidth
- Non-flat fading or (frequency selective fading)

Chapter 10

How to generate PDP Dataset using NYUSIM?

10.1 Generating PDP Information using NYUSIM

NYUSIM is a simulation tool which is based on measurement based channel modeling. The main strength of NYUSIM lies in generating PDP models for different simulation instants. The PDP generated using NYUSIM consists of a number of clusters and rays. There can be as many as 6 clusters which can be generated by NYUSIM base code. Each cluster contains 1-30 rays. The numbers of clusters and numbers of ray are randomly selected. The rays inside cluster represent multipath propagation of transmitted signal.

When the base code of NYUSIM is executed then a number of plots and output files are generated. Time taken by base code to complete this is around 15-20 seconds. For the purpose of obtaining PDP information only using NYUSIM we can neglect several plots and output text files which are irrelevant to us and only taking extra time in execution of complete program. Basically the PDP information in NYUSIM is saved in matrix variable named 'dirpdp_content'. This is the only relevant information. All the other code for generating different plots and text file is commented out with utmost care. As the base code itself is larger than 1000 lines of matlab script. If any variable declaration, calling function or equations for calculation are commented out which are needed in lower lines of matlab script then execution can't be completed. After commenting out the unnecessary code, the execution time for generating PDP dataset for a single simulation came out to be lower than 1 second. [15]

The matrix variable dirpdp_content consists of columns which corresponds to a particular data in PDP and rows corresponds to different time instants for different rays

which arrive at the receiver. The column of the matrix contains data in sequence as- Simulation Run Number, T-R Separation Distance, Time Delay(ns), Received Power(dBm), Phase(rad),

Azimuth AOD(degree), Elevation AOD(degree), Azimuth AOA(degree), Elevation AOA(degree), Path Loss(dB), RMS Delay Spread(ns). [2]

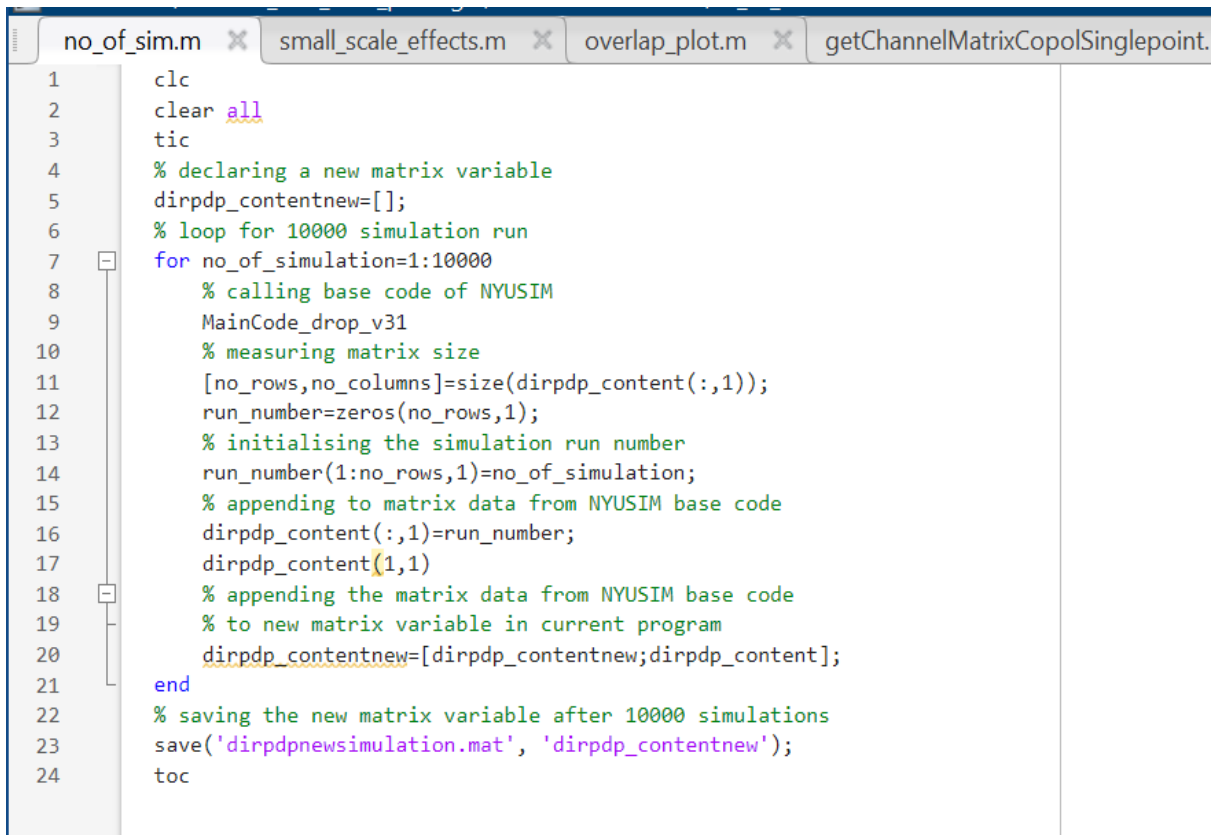
As explained in chapter 7 that NYUSIM can be used to show small scale effects. The PDP dataset is generated by drawing a conclusion from chapter 7 results that NYUSIM accounts for several moving reflectors due to which small scale effect, fading can be observed in results of Chapter 7. This conclusion is drawn because, when our T-R separation distance is fixed then still there are fading effects which can be observed in Fig.7.1.

So if we are able to run the NYUSIM base code a large number of times then we can have data of channel variations in terms of PDP. Here channel variations mainly refers to the presence of moving reflector inside the channel. In the following section a matlab script is given which is used to save 10,000 simulation run's PDP data.[13]

10.2 Matlab script for Generating PDP Dataset

Script 10.1 gives the matlab program to run the base code of NYUSIM 10^4 times. Also after running the script we have import the PDP information cell from Base Code to this running script. This information is assigned a corresponding simulation run number. After this it is appended to a matrix type variable. Every simulation's PDP information is appended to a certain matrix variable. In our case we have given this variable a name, 'dirpdp_contentnew'. In line 5 this variable is declared and after that a for loop is initialized for running 10^4 times. Inside this for loop, on line number 9 we called the NYUSIM base code. The PDP information is saved in cell type variable inside base code which is named 'dirpdp_content'. In line 5 size of this variable is measured. In line 12 a column vector of same number of rows as dirpdp_content is initialised. In line 14, this column vector is given the value of no_of_simulation. After this in line 16 it is appended to column 1 of dirpdp_content. After assigning simulation number we append this cell type matrix data to dirpdp_contentnew variable. The loop executes for 10^4 times similarly.

This variable is saved inside .mat file naming dirpdpnewsimulation.mat. This file is then accessed later to find Channel Matrix using Saleh-Valenzuela channel model.[16]



```
no_of_sim.m x small_scale_effects.m x overlap_plot.m x getChannelMatrixCopolSinglepoint.
1      clc
2      clear all
3      tic
4      % declaring a new matrix variable
5      dirpdp_contentnew=[];
6      % loop for 10000 simulation run
7      for no_of_simulation=1:10000
8          % calling base code of NYUSIM
9          MainCode_drop_v31
10         % measuring matrix size
11         [no_rows,no_columns]=size(dirpdp_content(:,1));
12         run_number=zeros(no_rows,1);
13         % initialising the simulation run number
14         run_number(1:no_rows,1)=no_of_simulation;
15         % appending to matrix data from NYUSIM base code
16         dirpdp_content(:,1)=run_number;
17         dirpdp_content(1,1)
18         % appending the matrix data from NYUSIM base code
19         % to new matrix variable in current program
20         dirpdp_contentnew=[dirpdp_contentnew;dirpdp_content];
21     end
22     % saving the new matrix variable after 10000 simulations
23     save('dirpdpnewsimulation.mat', 'dirpdp_contentnew');
24     toc
```

Script 10.1. Matlab Script to generate PDP Dataset for 10,000 instants.

Chapter 11

Channel Model and finding Channel Matrix

11.1 Channel Matrix

M number of transmitting antennas can be used to implement spatial diversity. The multiple data streams are obtained by the N number of receiving antennas. The available frequency band is used to transmit multiple data streams, this type of spatial multiplexing along with diversity, increases the link capacity. On the other side, MIMO systems with antenna diversity increase the link's dependability, as they introduce the concept of spatial diversity. The channel response matrix which is also known as Channel State Information (CSI) determines the performance of MIMO system and increases the capacity by large differences. The channel impulse response information changes more abruptly for the scenario of rapid fading channel and MIMO techniques are used to transform the variation in the channel to sub channels which are spatially separated. This indicates that the possibilities of utilizing this vast dataset of information in the construction of intelligent systems will increase with the addition of a dataset of channel state information or channel matrix.[13]

For a MIMO system configuration, first a test is done using, let's say a value of 1, by each of the transmitter antennas and this information gets altered while traveling inside the channel. This altered information is sensed at the receiving antennas. For example, we transmit voltage 1 at 1st Tx. antenna. Let's say, at the three receiver antennas following values are measured – [0.8, 0.7, 0.9]. This procedure for obtaining a channel matrix can be repeated at same time instants for multiple transmitting and receiving antennas. A channel matrix for each instant can be formed.

$$\begin{bmatrix} 1 & 0 & 0 \\ 0 & 0 & 0 \\ 0 & 0 & 0 \end{bmatrix} \rightarrow \begin{bmatrix} 0.8 & 0 & 0 \\ 0.7 & 0 & 0 \\ 0.9 & 0 & 0 \end{bmatrix}$$

The method which is explained above consists of transmitting antenna to send the data blindly to the receiver. At the receiver side a channel matrix is constructed. This is a open loop transmission scheme and is generally not very effective. As can be seen in the previous example that antenna 1 transmits a '1' and an amplitude of '0.8', '0.7' and '0.9' is received. This means that antenna 3 is receiving more efficiently and in that case antenna 1 and antenna 2 can be switched off which results in saving energy. This shows a system which uses a closed loop diversity scheme. The channel matrix example shown above only consists of only real number but in general channel matrix consists of complex elements. In those matrices the complex number(real+imaginary) describes both the link's amplitude and phase variation.[17]

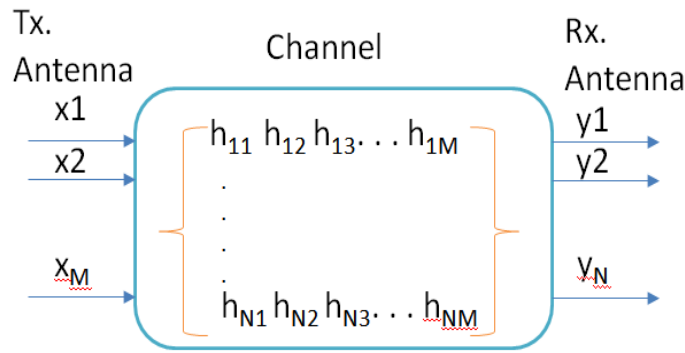


Fig. 11.1 Channel Matrix for M transmitting antenna and N receiving antennas

It is seen from Fig. 11.1 the receiver antennas in addition to receiving the LOS signal which is meant for corresponding antennas, a fraction of signal from multiple path of propagation is also received. And it is because of this reason that channel response is shown by using a Channel Matrix, h . The LOS path formed between antenna no.1 at the transmitting side and antenna no. 2 at the receiving side is shown by channel impulse response h_{11} . Similarly the channel impulse

response between antenna no. 1 at the transmitting side and the antenna no. 2 at the receiving side is represented by h_{12} and so on. This means that the size of the channel matrix is $N \times M$.

Consequently, using this justification, we can create an equation where the receive vector y is expressed as input vector x , noise vector n , channel transmission matrix H -

$$y = H.x + n \quad (11.1)$$

For a 2x2, MIMO configuration, the above given equation is written as -

$$y_1 = h_{11}.x_1 + h_{12}.x_2 + n_1 \quad (11.2)$$

$$y_2 = h_{21}.x_1 + h_{22}.x_2 + n_2 \quad (11.3)$$

This means that the receiver has to carry out the operation given in equation 11.2 and 11.3. and determine what is received in a certain channel condition.

11.2 Saleh-Valenzuela Channel Model

Saleh and Valenzuela described a new channel model based on the Power Delay Profile(PDP) of the received power in [16]. The findings using which they proposed a new channel model are related to PDP. In the PDP there are multiple clusters present, and each cluster is having multiple rays in the power delay profile.

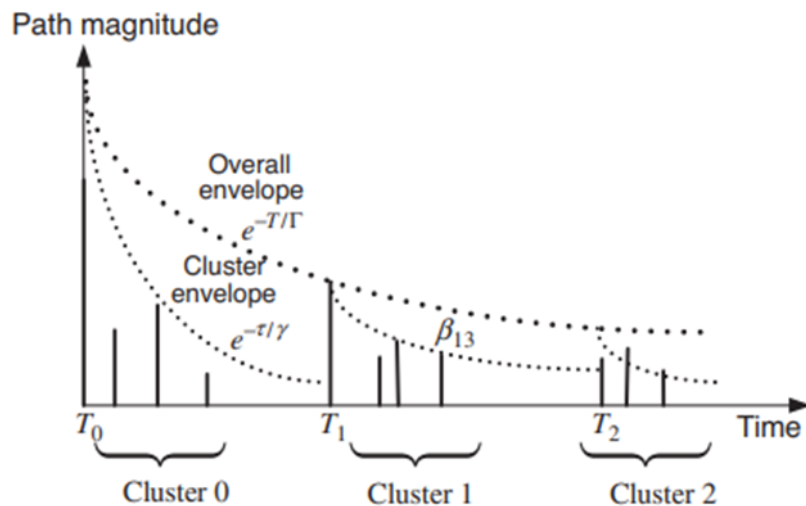


Fig. 11.2 Multiple clusters from Multipath propagation of transmitted signal

S-V channel model is shown in Fig. 11.2 with a number of rays, a set of these rays are related with a single corresponding cluster. The times of arrival for each cluster and all the rays present in each cluster follows an independent Poisson process, as given in [17]. Therefore we can say that in fig. 11.2 each ray amplitude is separated in time domain by a certain distance. Each of these distances are arbitrary i.e. each ray is distanced somewhat randomly rather than at a distance that is a multiple of the sampling period.

Let's consider $\beta_{r,m}$ and $\theta_{r,m}$ denotes the amplitude and phase of the r_{th} ray in the m_{th} cluster, respectively. Then a channel impulse response in [17] is given as -

$$h(t) = \sum_{m=0}^{\infty} \sum_{r=0}^{\infty} \beta_{r,m} \cdot e^{j\theta_{r,m}} \delta(t - T_m - \tau_{r,m}) \quad (11.4)$$

where, T_m is the arrival time of the m_{th} cluster

$\tau_{r,m}$ is the arrival time of the r_{th} ray in m_{th} cluster

In the equation 11.4, $\theta_{r,m}$ is considered as a random variable that follows uniform distribution over $[0, 2\pi)$ and $\beta_{r,m}$ is an independent random variable which is Rayleigh Distributed -

$$f_{\beta_{r,m}}(\beta_{r,m}) = (2\beta_{r,m}/\underline{\beta_{r,m}^2}) e^{-\beta_{r,m}^2/\underline{\beta_{r,m}^2}} \quad (11.5)$$

where, $\underline{\beta_{r,m}^2}$ is the average power of the r_{th} ray in the m_{th} cluster.

As shown in Fig. 11.2 the power decays exponentially for rays and clusters, we can establish an exponential relationship of the first ray with the rest of the rays. If the first ray's average power present in the first cluster is available then the average power of all the other rays can be found out with the help of exponential relationships with the first ray. It means that we can find all the Rayleigh channel coefficients using (11.5). Without losing generality we can set the power of the first ray present in the first cluster to one if a path loss is not taken into account. As there can be infinite no. of propagation path so there can be infinite number of rays and clusters in the channel impulse response of Equation 11.4, but we neglect many rays whose average power is lower than a threshold value. Therefore, we limit the number of clusters and rays to M and R, respectively. Meanwhile, a log-normal random variable \mathbf{X} , that is, $20\log_{10}(\mathbf{X})$

$\sim \mathcal{N}(0, \sigma_x^2)$ can be introduced to Equation 11.4, so as to reflect the effect of long-term fading in [17] as -

$$h(t) = X \cdot \sum_{m=0}^{\infty} \sum_{r=0}^{\infty} \beta_{r,m} \cdot e^{j\theta_{r,m}} \delta(t - T_m - \tau_{r,m}) \quad (11.6)$$

11.3 Matlab Script for finding Channel Matrix

The S-V model is used in the script for finding a channel impulse response using particular PDP corresponding to a certain time instant. In the script as can be seen from line no. 3 that first the BasicParameters.mat file is loaded which contains the information about channel conditions and number of transmitting and receiving antennas.

After that in line 14 dirpdpnewsimulation.mat file is loaded which contains the matrix variable dirpdp_contentnew. This cell type matrix contains data about the PDP for different time instants, in our case 10,000 instants. Line 18 and 19 are used to remove any lines in the matrix which contain NaN as they can corrupt the PDP dataset.

There are 10,000 simulation runs, each containing its random PDP information. Each simulation run is given a number. Line 23 take unique simulation number as input to SimNum variable i.e. taking data from column 1 of the dirpdp_contentnew matrix. In line 25 phase data from the variable dirpdp_contentnew is taken out i.e. column 5th of the PDP dataset.

After initializing several variable, a for loop is initialized in the line 31 to select through every simulation number PDP dataset. For every simulation number specific data about a set of rays is present. Another for loop is initialized in the line 33 for determining if different sub-carriers are used. The for loops in line 35 and 36 determines the matrix size according to the number of transmitting and receiving antennas. Equation 11.4 is then implemented in the line 38 and 39. After calculating each instant's CIR, it is appended to a 'A' matrix variable and then to HF_pvs variable. This HF_pvs is in cell format and it is converted to matrix format for taking its fft. The resulting matrix dataset is then saved in the file hmatrixfile.mat and the phase data in phase_dis.mat.

```

getChannelMatrixCopolSinglepoint.m  no_of_sim.m  small_scale_effects.m  overlap_plot.m  normalised_histogram.m
1      clc
2      clear all; close all; tic
3      load('BasicParameters.mat'); % load the output data file containing the basic channel parameters
4      f = BasicParameters.Frequency; % center carrier frequency
5      RFBW = BasicParameters.Bandwidth; % RF bandwidth
6      Nt = BasicParameters.NumberOfTxAntenna; % number of transmit antenna elements
7      Nr = BasicParameters.NumberOfRxAntenna; % number of receive antenna elements
8      dTxAnt = BasicParameters.TxAntennaSpacing; % spacing between adjacent transmit antenna
9      % elements with respect to the wavelength
10     dRxAnt = BasicParameters.RxAntennaSpacing; % spacing between adjacent receive antenna
11     % initialising path for the generated dataset
12     filename='dirpdpnewsimulation.mat';
13     foldername='D:\NYUSIM_V31_WIN_package\NYUSIM Base Code';
14     myfile=fullfile(foldername,filename);
15     load(myfile); % load the output data file containing the channel impulse response parameters
16
17     % Remove NaN lines
18     nanInd = isnan(dirpdp_contentnew(:,3));
19     dirpdp_contentnew(nanInd,:) = [];
20
21     % Find the unique simulation number to obtain the channel matrix for each of
22     % the TX-RX location pairs
23     SimNum = unique(dirpdp_contentnew(:,1));
24     % find the phase for particular arriving ray from column 5
25     phase_dis=dirpdp_contentnew(:,5);
26     j = sqrt(-1);
27     f_sub = f;
28     Hf_pvs = cell(length(f_sub),length(SimNum));
29
30     % initialising matrix variable
31     A={};
32     for id = 1:length(SimNum)
33         clear Idx; Idx = find(dirpdp_contentnew(:,1)==SimNum(id));
34         for q = 1:length(f_sub)
35             Hf_temp = zeros(Nr,Nt);
36             for w = 1:Nr
37                 for y = 1:Nt
38                     % using saleh-valenzuela channel model
39                     Hf_temp(w,y) = sum(sqrt(10.^(dirpdp_contentnew(Idx,4)./10)) ...
40                                     .*exp(1i.*dirpdp_contentnew(Idx,5)));
41                     % appending to A
42                     A = [A; Hf_temp];
43                 end
44             end
45             Hf_pvs{q,id} = Hf_temp;
46         end
47     end
48     % converting from cell to matrix format
49     Hf_time=cell2mat(Hf_pvs);
50     % inverting the operation done in line 42 of phase multiplication
51     hf_freq=fft(Hf_time);
52     % saving the hmatrix and phase data of arriving rays
53     save('hmatrixfile.mat', 'hf_freq');
54     save('phase_dis.mat', 'phase_dis');
55     toc

```

Script 11.1. Matlab Script for finding Channel Matrix

Chapter 12

Verifying the Results

Up to this point we have generated a channel matrix in a certain environment. In the Chapter 8, Rayleigh Distribution, we have already set the conditions by assuming the channel variables. These are -

- in the channel moving reflectors are present
- multipath is present
- transmitting antenna radiating power at a certain frequency without mobility
- receive antenna receiving the power at a certain point
- i.e. T-R separation constant

The transmitted signal is said to be affected by rayleigh fading which is present in the channel because of moving reflectors in the channel. This is already explained theoretically in Chapter 8, Rayleigh Distribution along with the mathematical aspect of Rayleigh Distribution. It was also said that the phase of received signal will change randomly but with uniform distribution between the range 0 to 2π .

The above given channel conditions are set in the matlab base script of NYUSIM. These are set by changing several script variable in MainCode_drop_v31.m. The values of different variables are given in the Table 12.1.

As we have already said that up till this chapter we have a channel matrix. This channel matrix is found out using Saleh-Valenzuela channel model. Each column in this row vector represent the corresponding channel condition in complex form for SISO system. There are 10,000 such column and it can be said to contain all the variations in the channel. This complex row vector is stored in the file hmatrixfile.mat.

Table 12.1. Channel Parameters entered in NYUSIM

Channel Parameters	
Frequency (GHz)	28
Tx Power (dBm)	40
Scenario	UMi
Environment	NLOS
T-R Separation (m)	50,100
BS height(m)	20,40
μ T height(m)	1.5
Pressure (mbar)	1013.25
Humidity (%)	50
Temperature (°C)	30
Foliage	Yes
Distace within Foliage(m)	15
O2I Penetration Loss	Yes
No. of BS elements	1
No. of μ T elements	1

For verifying whether the generated dataset of channel matrix, using the dataset of 10,000 simulations run on NYUSIM, is correct or not, we have written a matlab script with the name `normalized_histogram.m`. This script gives the characteristics of the channel matrix for the SISO system in terms of histogram, pdf and plots which shows deep fading points at various points in time.

Script 12.1 is named as `normalized_histogram.m`. Each line has a comment written over it to describe its function. As shown in line 4 and 5 the two files which are mentioned in Chapter 11 are loaded in this script, namely, `hmatrixfile.mat` and `phase_dis.mat`. In line 8 histogram of `phase_dis` dataset is saved in variable 'h' and in line 9 probability values using Normalization and pdf attribute of function `histcount` is saved in variable 'p'.

```

normalised_histogram.m x getChannelMatrixCopolSinglepoint.m x no_of_sim.m x small_scale_effects.m
1      clc
2      clear all; close all;
3      % loading the hmatrix file and phase data file
4      load('hmatrixfile.mat');
5      load('phase_dis.mat')
6      % plotting the histogram of phase data
7      figure(1);
8      h = histogram(phase_dis,50);
9      p = histcounts(phase_dis,50,'Normalization','pdf');
10     % plotting the pdf of phase
11     figure(2);
12     binCenters = h.BinEdges + (h.BinWidth/2);
13     stem(binCenters(1:end-1), p, 'r-')
14     xlabel('phase in radians from 0 to 2pi(6.28)');
15     ylabel('probability');
16     title('pdf of phase');
17     % measuring size of h matrix
18     [r,c]=size(hf_freq);
19     for i=1:c
20         A=[real(hf_freq(1,i)),imag(hf_freq(1,i))];
21         % for finding resultant of each complex CIR
22         resultant(i)=sqrt(A(1,1)^2 + A(1,2)^2);
23     end
24     % normalizing the resultant data
25     h_normalized=resultant/(sqrt(var(resultant)));
26     % plotting normalized values histogram
27
28     figure(3);
29     histogram(h_normalized);
30     xlabel('normalized resultant values(h_normalized)');
31     ylabel('number of occurence');
32     title('histogram for generated channel model');
33     [count1, xvlaues]=hist(h_normalized,1000);
34     % plotting proof of randomness in channel
35     figure(4);
36     plot(10*log10(h_normalized(1:100)));
37     xlabel('instantaneuos time');
38     ylabel('normalised amplitude of channel output');
39     title('randomness in channel from one time instant to other');
40     cir=10*log10(h_normalized);
41     % plotting the histogram first for finding pdf of normalized resultant data
42     figure(5);
43     h = histogram(h_normalized,50);
44     p = histcounts(h_normalized,50,'Normalization','pdf');
45     % plotting the pdf using histogram of normalized resultant data
46     % also correcting number of bins in histogram command
47     % to plot smooth pdf curve with corresponding ranges
48     figure(6);
49     binCenters = h.BinEdges + (h.BinWidth/2);
50     plot(binCenters(1:end-1), p, 'r-')
51     xlabel('instantaneous value of the resultant amplitude');
52     ylabel('probability');
53     title('pdf of h(t)');

```

Script 12.1. Matlab Script for plotting PDF of normalized h matrix dataset of SISO system

In line 12 binCentres are calculated by adding half bin width to bin edges. These bin width and bin edges are accessed using the variable h. After this the binCenters and p are plotted on the x and y axis respectively using the stem function in line 13. (as shown in Fig. 12.3)

In line 18, first the size of the h-matrix saved in hmatrixfile.mat is measured. After this a for loop is initialized to run for as many times as there are a number of columns in the h_matrix.

Inside this for loop, in line 22, resultant for each complex element of the matrix is calculated.

In line 25, the resultant variable is normalized by dividing the whole data with $\sqrt{\text{var}(\text{resultant})}$ (i.e square root of variance of resultant). The normalized values are saved

in the h_normalized variable. Histogram for these values is also plotted and given in Fig. 12.1.

From line 35 to 38 channel response is plotted by converting the resultant values to dB and fading points along with randomness in channel can be observed. After this the pdf for the histogram of h_normalized is calculated. In line 42 histogram of phase_dis dataset is saved in variable 'h' and in line 43 probability values using Normalization and pdf attribute of function histcount is saved in variable 'p'. In line 48 binCentres are calculated by adding half bin width to bin edges. These bin width and bin edges are accessed using the variable h. After this the binCenters and p are plotted on x and y axis respectively using plot function in line 49.

As the normalized resultant is saved in the variable h_normalized which is an array and contains 10,000 values. The histogram of the dataset present in the variable h_normalized is shown in Fig. 12.1. As it is clearly seen in the Fig. 12.1. that this

plot can directly be compared with the pdf of Rayleigh Distribution in Chapter 8. This is considered a major result because it proves the assumptions which were made initially. This also tells us that the program used for h-matrix dataset generation and PDP dataset generation can be further used to generate different channel models for different input parameters.

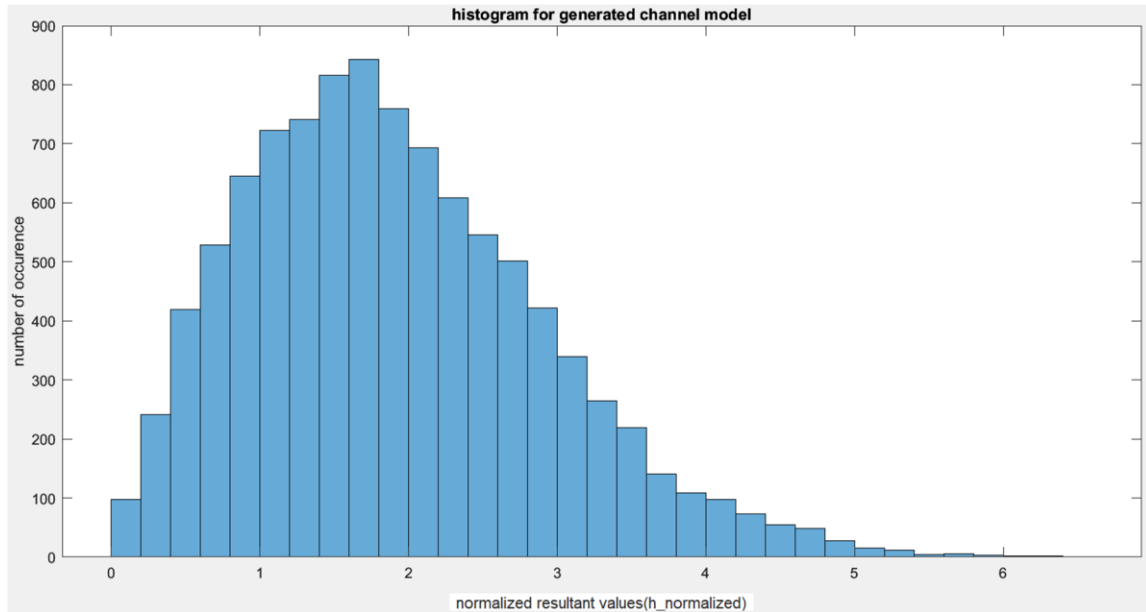


Fig 12.1. Histogram for generated channel model

The pdf of the above given histogram can be found easily by dividing the number of values coming in a range by the total number of values as explained in the program above. The pdf for the generated channel model is given in Fig. 12.2.

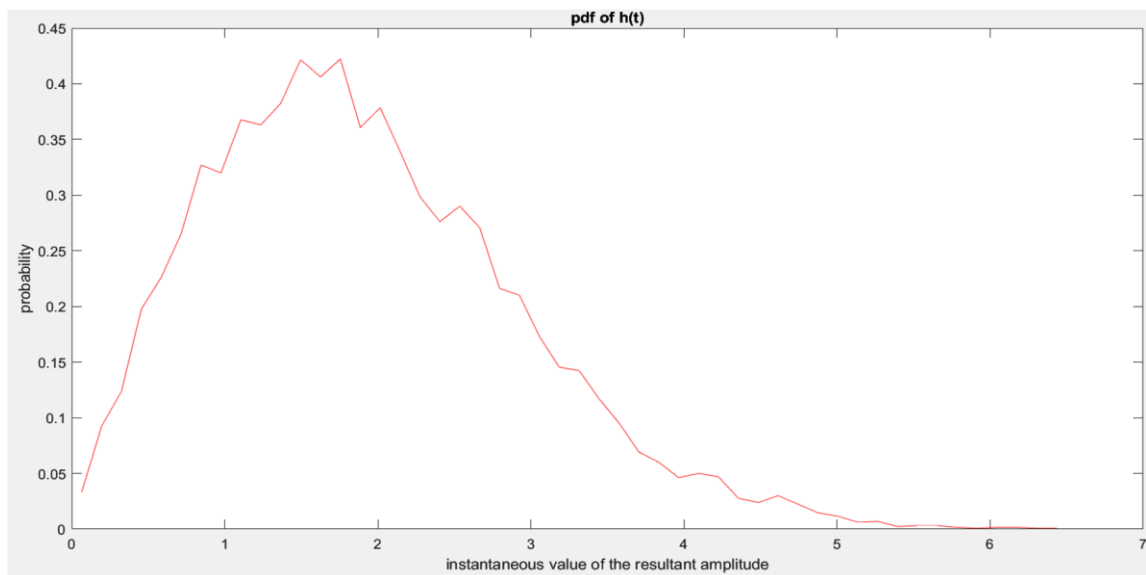


Fig 12.2. PDF for generated channel model

As explained theoretically in chapter 8 that in case of rayleigh fading the phase of incoming multipath signals arriving at the receiver is uniformly distributed between the range 0 to 2π . This is shown in the Fig. 12.3.

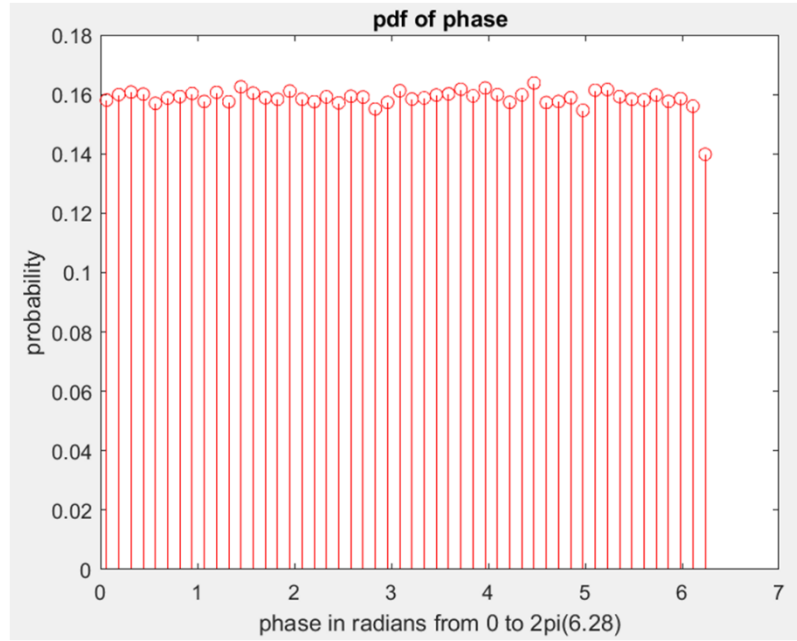


Fig. 12.3. PDF for phase of the amplitude received

These results imply that the channel matrix dataset which is obtained using the dataset of the different multipath signals arriving at the receiver is coinciding with the theoretical results presented in chapter 8 and chapter 9. Given channel model is obtained with application of mmWave frequency in SISO communication system.

Another result that can be obtained using modified scripts of NYUSIM along with proposed scripts is given in Fig. 12.4. It shows that when the channel parameter is changed, for example if T-R separation is changed from 50 m to 100 m then the pdf of the channel model changed slightly and randomly. This gives rise to one more application of the proposed dataset that using data of some changes in the channel the modified NYUSIM program can predict the channel impulse response dataset. The script for these 2 overlapping plots is written separately with the name `overlap_plot.m`. The program is shown in Script 12.2.


```

overlap_plot.m x small_scale_effects.m x no_of_sim.m x getChannelMatrixCopolSinglepoint.m
1      clc
2      clear all; close all;
3      % loading h matrix file dataset file
4      filename='hmatrixfile.mat';
5      foldername1=['D:\NYUSIM_V31_WIN_package\project related ' ...
6      'files\28Ghz rayleigh channel 10000 simrun without NAN final'];
7      foldername2=['D:\NYUSIM_V31_WIN_package\project related ' ...
8      'files\28Ghz rayleigh channel 10000 simrun without NAN ' ...
9      'final tx height 40 sep 100'];
10     % loading other h matrix dataset file
11     myfile1=fullfile(foldername1,filename);
12     load(myfile1);
13     % measuring size of h matrix loaded first
14     [r,c]=size(hf_freq);
15     for i=1:c
16         A=[real(hf_freq(1,i)),imag(hf_freq(1,i))];
17         % calculating resultant of complex data
18         resultant(i)=sqrt(A(1,1)^2 + A(1,2)^2);
19     end
20     % normalizing the resultant
21     h_normalized=resultant/(sqrt(var(resultant)));
22     % plotting its histogram
23     figure(1);
24     h = histogram(h_normalized,50);
25     p = histcounts(h_normalized,50,'Normalization','pdf');
26     % plot its pdf using corresponding bins
27     figure(2);
28     binCenters = h.BinEdges + (h.BinWidth/2);
29     plot(binCenters(1:end-1), p, 'r-')
30     xlabel('instantaneous value of the resultant amplitude');
31     ylabel('probability');
32     title('pdf of h(t)');
33
34     hold on
35     % plotting proof of randomness in channel
36     figure(3);
37     plot(10*log10(h_normalized(1:100)));
38     xlabel('normalised amplitude of channel output');
39     ylabel('instantaneous time');
40     title('randomness in channel from one time instant to other');
41     hold on
42
43     myfile2=fullfile(foldername2,filename);
44     load(myfile2);
45     % measuring size of h matrix loaded after the first one
46     [r,c]=size(hf_freq);
47     for i=1:c
48         A=[real(hf_freq(1,i)),imag(hf_freq(1,i))];
49         % calculating resultant of second h matrix
50         resultant(i)=sqrt(A(1,1)^2 + A(1,2)^2);
51     end
52     % normalizing the resultant
53     h_normalized=resultant/(sqrt(var(resultant)));
54     % plotting its histogram
55     figure(4);
56     h = histogram(h_normalized,50);
57     p = histcounts(h_normalized,50,'Normalization','pdf');
58     % plot its pdf over the first plot
59     binCenters = h.BinEdges + (h.BinWidth/2);
60     figure(2);
61     plot(binCenters(1:end-1), p, 'b-')
62     % plotting proof of randomness over the first plot
63     figure(3);
64     plot(10*log10(h_normalized(1:100)));

```

Script 12.2. overlap_plot.m

First the channel matrix dataset for 50m T-R separation is saved in a particular folder and then another dataset for 100m T-R separation is saved in the same folder. A matlab script is written to load both the dataset. Their resultant is calculated separately and after this both are normalized. Plotting the pdf of the normalized dataset simultaneously is shown in Fig. 12.4.

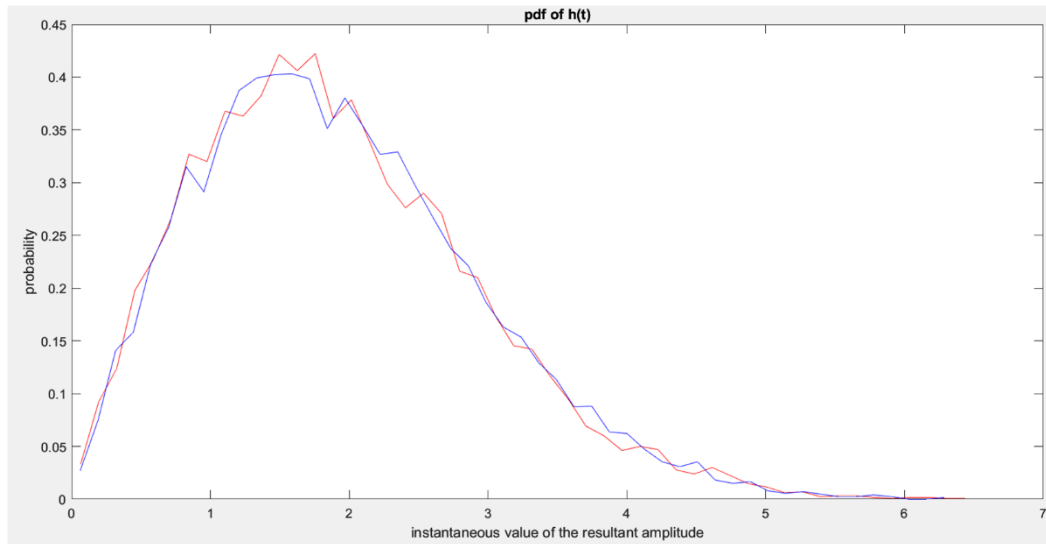


Fig. 12.4. PDF for generated channel model for different T-R separation

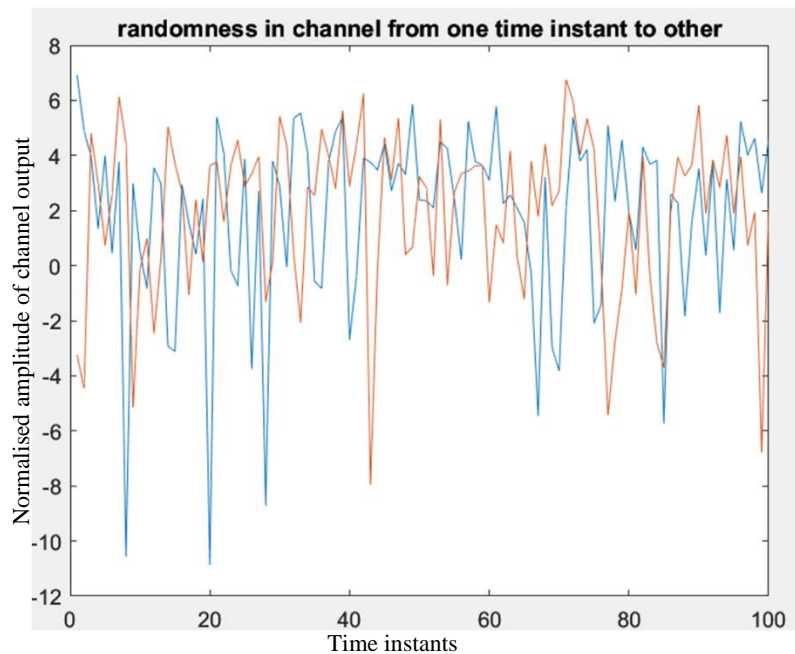


Fig. 12.5. Random variations in channel as shown by overlapping resultant of CIR for 2 conditions

Verification of randomness of received power at a single point from one time instant to another is shown in Fig. 12.5. The variations in the given channel from time to time can be shown by taking logarithm to the base 10 of the resultant channel matrix. These random variations arise as there are several moving reflectors which change their position from time to time. In Fig.12.5 only some samples are shown to avoid confusion. The samples where the signal gets deeply faded is shown in the figure. For two different conditions of the channel we can see that deep fades occur at different time instants.

This is very useful in case of communication. As the transmitted signal only gets multiplied by channel impulse response and additive white gaussian noise(AWGN) gets added to the transmitted signal. This suggests that we can have unknown data with known Flat Fading characteristics. In this situation we can say we have perfect channel estimation.

Chapter 13

Conclusion

In the initial part, chapter 2, path loss model is studied which is implemented inside NYUSIM and is mainly dependent on Path Loss exponent and Friis Free space equation. The path loss came out to be as high as 130dB for T-R separation of around 400 m even when other things such as Transmitter-Receiver height, foliage loss and penetration loss is not considered in the overall path loss model. This directly signifies to form a small cell size so that mmWave signal can overcome this Path Loss..In small cells the signal will travel less distances because of increasing attenuation with larger distances. Therefore, less power than in the case of Larger cell will be required.

In chapter 3 data collected for the effect of rain rate on the transmitted signal is discussed. For the ranges from a few hundreds of meters up to 30km, the power used for transmitting varies between 10 Watts to 50 Watts. Also the desired power should be 18dB i.e 64 times more than the interference power from other cells only then a faithful transmission of message signal over mmWave spectrum can be processed. In the data, the best case and best possibility measure is taken i.e. low rain rate and directive antenna but still the received signal strength goes as low as -50dBm(for tx. Power 30dBm). It translates to radiating more power but as cell size will already be reduced this large amount of power translates to more co-channel interference and it will also have adverse effects on all life. Effect of foliage and penetration loss also lowers the received signal power which is shown in chapter 4 and chapter 5. For ignoring it the channel should contain multiple links so that the number of foliage elements and walls present inside the channel between 2 links could be reduced which can enhance the power received but the infrastructure cost for this could be too high. Proper measures should be taken to reduce the infrastructure cost.

Further the effect of co-polarized and cross-polarized antennas are also studied in chapter 6 and it suggests that the polarization effect changes the received power. PLE(Path Loss Exponent) for omni-directional antenna is less than that for directional antenna hence the path loss comes out to be high when cross-polarization with directional antenna is used. But the received power is low when cross-polarization is used. The results are also useful for showing that antenna radiation pattern effects Path Loss and PLE. In fact it is capable to increase or decrease the propagation path loss along with PLE.

In chapter 7 it is found that NYUSIM is merely a database and plotting program which gives output for a certain set of channel conditions. If a LOS condition is used inside NYUSIM then only attenuation due to Friis Free Space equation is incorporated but when NLOS condition is selected then multipath due to moving reflectors or changing channel conditions comes into play. Because of this small scale effects play a major role in determining the received power. As moving reflectors move by order of the wavelength there are fast fluctuations in the magnitude of received signal. It is shown in chapter 7 using fig. 7.1.

Chapter 8 and 9 deals with realizing the fact that a large amount of data can be retrieved from NYUSIM using its base code. Understanding this data requires a knowledge of the power delay profile of the received signal. Along with PDP, the distribution, which the amplitude of received signal follows, is to be studied which is covered in both chapter 8 and chapter 9. This data can be found using the explanations provided in chapter 10. The channel model can be calculated from the given dataset in chapter 10. Saleh Valenzuela channel model is used to build a matlab script as shown in chapter 11 to realize channel matrix. The verification of the proposed channel matrix is done by plotting separate characteristics of the channel conditions and verifying them with the theoretical results obtained in Chapter 8 and Chapter 9. There are different uses of the Generated dataset of channel matrix. Some of them are listed as:-

- Extensive research for channel prediction is popular in the field of 5G and 6G communication.
- Machine Learning can give an extension to the current state of our project as it can help in predicting CIR for changes in the channel.
- The predicted channel will reduce the need of pilot signal for estimating CIR.
- The modified program using NYUSIM for dataset generation can be used to generate data for various environments.
- It reduces the need for costly channel measurement projects.
- The given program can not only be used for SISO channel measurements but also for MIMO channel measurements.
- The proposed dataset for channels can be used to find Average Fade Duration and Outage Probability.
- Link performance is an important factor(i.e. BER) in a SISO system.
- System performance (i.e. latency & throughput) can be found using our dataset in a multi-user scenario.

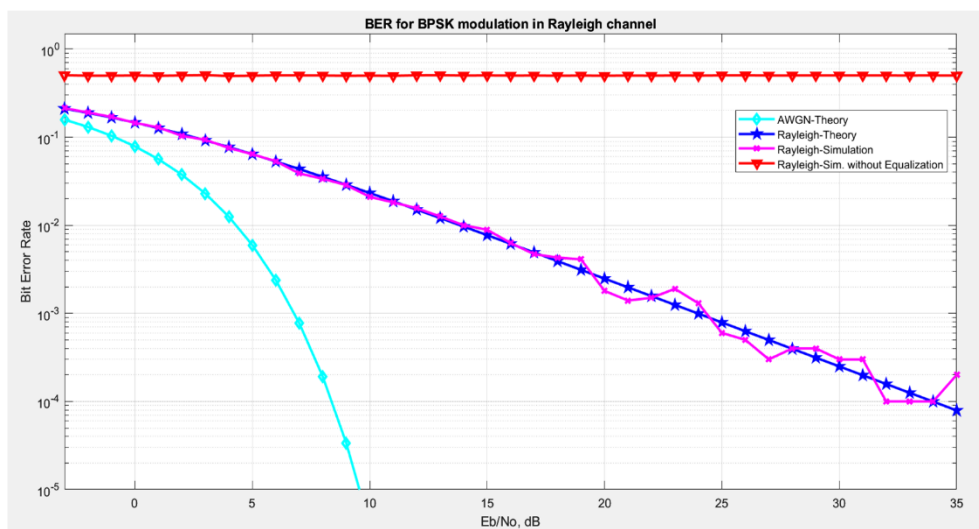


Fig. 13.1 BER for BPSK modulation in the generated dataset for Rayleigh Channel

One application of the generated dataset of channel matrix is given in Fig. 13.1. where the theoretical performance of BPSK in rayleigh channel using proposed data is shown.

References

- [1] T. S. Rappaport, S. Sun, R. Mayzus, H. Zhao, Y. Azar, K. Wang, G. N. Wong, J. K. Schulz, M. Samimi, and F. Gutierrez, "Millimeter wave mobile communications for 5G cellular: It will work!" *IEEE Access*, vol. 1, pp. 335–349, 2013.
- [2] M. K. Samimi and T. S. Rappaport, "3-D millimeter-wave statistical channel model for 5G wireless system design," *IEEE Transactions on Microwave Theory and Techniques*, vol. 64, no. 7, pp. 2207–2225, Jul. 2016.
- [3] Shu Sun, Theodore S. Rappaport and Sundeep Rangan, "Propagation Path Loss Models for 5G Urban Micro- and Macro-Cellular Scenarios" *IEEE 83rd Vehicular Technology Conference (VTC Spring)*, 2016, DOI: 10.1109/VTCSpring.2016.7504435.
- [4] P. Papazian and Y. Lo, "Seasonal variability of a local multi-point distribution service radio channel," in *IEEE Radio and Wireless Conference*, 1999, pp. 211–214.
- [5] M. Chavero, V. Polo, F. Ramos, and J. Marti, "Impact of vegetation on the performance of 28 GHz LMDS transmission," in *IEEE MTT-S International Microwave Symposium Digest*, vol. 3, June 1999, pp. 1063–1066.
- [6] T. S. Rappaport and S. Deng, "73 GHz wideband millimeter-wave foliage and ground reflection measurements and models," in *2015 IEEE International Conference on Communication Workshop (ICCW)*, Jun. 2015, pp. 1238–1243.
- [7] Aalto University, AT&T, BUPT, CMCC, Ericsson, Huawei, Intel, KT Corporation, Nokia, NTT DOCOMO, New York University, Qualcomm, Samsung, University of Bristol, and University of Southern California, "5G channel model for bands up to 100 GHz," 2016, Oct. 21.
- [8] Shihao Ju, Shu Sun, and Theodore. S. Rappaport, "NYUSIM USER MANUAL", 2022, Version 3.1 Copyright 2016 – 2022 New York University and NYU WIRELESS.
- [9] Joaquim Amandio Azevedo, Filipe Adgar Santos, Tony Andres Sousa, Jenny Manuela Agrela, "Impact of Antenna Directivity on path loss for different propagation environments", 2015, DOI: 10.1049/iet-map.2015.0194.
- [10] T. Manabe, K. Sato, H. Masuzawa, K. Taira, T. Ihara, Y. Kasashima, and K. Yamaki, "Polarization dependence of multipath propagation and high-speed transmission characteristics of indoor millimeter-wave channel at 60 ghz," *IEEE Transactions on Vehicular Technology*, vol. 44, no. 2, pp. 268–274, 1995.
- [11] Zekri, A.B. and Ajgou, R. Towards 5G: A study of the impact of antenna polarization on Statistical Channel Modeling, Sustainable Engineering and Innovation. 2022.
- [12] Mathuranathan, *Wireless Communication Systems in Matlab (second Edition)* ISBN:979-8648350779.
- [13] R. Ilyas, A. Malik, A. A. Alammari and M. Sharique, "5G and mmWave MIMO Channel Models: Simulations and Analysis," 2021 Sixth International Conference on Wireless Communications, Signal Processing and Networking (WiSPNET), Chennai, India, 2021, pp. 435-440, doi: 10.1109/WiSPNET51692.2021.9419444.

- [14] A. Tkac, V. Wieser and S. Pollak, "Calculation of impulse response in Rician and Rayleigh channel," 2012 ELEKTRO, Rajcke Teplice, Slovakia, 2012, pp. 99-102, doi: 10.1109/ELEKTRO.2012.6225580.
- [15] M. K. Samimi and T. S. Rappaport, "Local multipath model parameters for generating 5G millimeter-wave 3GPP-like channel impulse response," 2016 10th European Conference on Antennas and Propagation (EuCAP), Davos, Switzerland, 2016, pp. 1-5, doi: 10.1109/EuCAP.2016.7481410.
- [16] A.A.M. Saleh, R. Valenzuela, "A statistical model for Indoor Multipath Propagation" in 1987 IEEE Journal on Selected Areas in Communications, vol. 25, no. 10, pp. 3151-3155, Oct. 2021, doi: 10.1109/JSAC.1987.1146527.
- [17] Cho, Y. S., Kim, J., Yang, W. Y., & Kang, C. G. (2010). *MIMO-OFDM Wireless Communications with MATLAB*. Wiley Online Library, doi: 10.1002/9780470825631.
- [18] William C. Y. Lee. *Wireless and Cellular Communications*: Vol. 821 pages (3rd, ed.). (2006). McGraw-Hill Education.
https://books.google.co.in/books/about/Wireless_and_Cellular_Communications.html?id=oxofAQAAIAAJ&redir_esc=y.
- [19] Y. Xing, T. S. Rappaport, and A. Ghosh, "Millimeter Wave and Sub-THz Indoor Radio Propagation Channel Measurements, Models, and Comparisons in an Office Environment," in IEEE Communications Letters, vol. 25, no. 10, pp. 3151-3155, Oct. 2021, doi: 10.1109/LCOMM.2021.3088264.
- [20] Goldsmith, A. (2005). *Wireless Communications*. Cambridge University Press, doi: 10.1017/cbo9780511841224.